SECURITY CLASSIFICATION OF THIS PAGE

REPORT DOCUMENTATION PAGE

Form Approved
OMB No. 0704-0188

1a. REP Un / a. SEC	1b RESTRICTIVE MARKINGS
AD-A215 679	3. DISTRIBUTION / AVAILABILITY OF REPORT Approved for public release; distribution unlimited
2b. DE	
4. PERFORMING ORGANIZATION REPORT NUMBER(S) Final Report	5. MONITORING ORGANIZATION REPORT NUMBER(S) AFOSR-TR- 89-1348
6a. NAME OF PERFORMING ORGANIZATION The Pennsylvania State University	6b. OFFICE SYMBOL (If applicable)
6c. ADDRESS (City, State, and ZIP Code) Materials Research Laboratory University Park, PA 16802	7a. NAME OF MONITORING ORGANIZATION Air Force Office of Scientific Research
	7b. ADDRESS (City, State, and ZIP Code) Bolling Air Force Base Washington, DC 20332
8a. NAME OF FUNDING / SPONSORING ORGANIZATION Air Force Office Of Scientific Research	8b. OFFICE SYMBOL (If applicable)
	9 PROCUREMENT INSTRUMENT IDENTIFICATION NUMBER Contract F49620-88-C-0134
8c. ADDRESS (City, State, and ZIP Code) Bolling Air Force Base Washington, DC 20332	10. SOURCE OF FUNDING NUMBERS PROGRAM ELEMENT NO. / PROJECT NO. / TASK IO / WORK UNIT ACCESSION NO.

11. TITLE (Include Security Classification)

Crystallization of Nanocomposite Glasses Made by the SSG Process

12. PERSONAL AUTHCR(S)
Rustum Roy and Sridhar Komarneni

13a. TYPE OF REPORT	13b. TIME COVERED	14. DATE OF REPORT (Year, Month, Day)	15. PAGE COUNT
Final Report	FROM 9/1/88 TO 8/31/89	October 18, 1989	82

16. SUPPLEMENTARY NOTATION

17. COSATI CODES			18. SUBJECT TERMS (Continue on reverse if necessary and identify by block number)
FIELD	GROUP	SUB-GROUP	

19. ABSTRACT (Continue on reverse if necessary and identify by block number)

(See page iv.)

20. DISTRIBUTION / AVAILABILITY OF ABSTRACT	21. ABSTRACT SECURITY CLASSIFICATION
☐ UNCLASSIFIED/UNLIMITED ☒ SAME AS RPT ☐ DTIC USERS	Unclassified
22a. NAME OF RESPONSIBLE INDIVIDUAL	22b. TELEPHONE (Include Area Code) / 22c. OFFICE SYMBOL

DD Form 1473, JUN 86 *Previous editions are obsolete.* SECURITY CLASSIFICATION OF THIS PAGE

COMPLETED PROJECT SUMMARY

TITLE: Crystallization of Nanocomposite Glasses Made by the SSG Process

PRINCIPAL INVESTIGATORS: Professors Rustum Roy and Sridhar Komarneni
Materials Research Laboratory
The Pennsylvania State University
University Park, PA 16802-4801

INCLUSIVE DATES: 1 September 1988 — 31 August 1989

CONTRACT/GRANT NUMBER: ~~AFOSR~~ F49620-88-C-0134

COSTS AND FY SOURCE: $143,000.

SENIOR RESEARCH PERSONNEL: Professor C.G. Pantano
Dr. Ulgaraj Selvaraj

JUNIOR RESEARCH PERSONNEL:

Ann M. Kazakos
Nancy Wlodarczyk
Hanxi Zhang

PUBLICATIONS:

"Multiphasic Nanocomposite Sol-Gel Processing of Cordierite," A.K. Kijowski, S. Komarneni and R. Roy, in Better Ceramics Through Chemistry, Vol. III (C.J. Brinker, D.E. Clark and D.R. Ulrich, eds.), Mat. Res. Soc. Proc., Pittsburgh, PA, pp. 245-250 (1988).

"Synthesizing New Materials to Specification," R. Roy, Solid State Ionics 32/33, 3-22 (1989).

ABSTRACT OF OBJECTIVES AND ACCOMPLISHMENTSÚ

The following two research phases were planned:

(1) Explore the role of solid state epitaxy in the crystallization of glass compositions to make glass ceramics.

(2) Extend the validity of solid state epitaxy by the crystallization of gel films on single crystals.

The nanocomposite xerogel route was utilized to attempt to make a universal glass-ceramic with controllable crystallization. Isostructural seeding of cordierite glass led to a lowering in crystallization temperature due to epitaxy just as in the nucleated crystallization of ceramics.

In an attempt to prove the validity of the solid-state epitaxy, single crystals and polycrystalline substrates of alumina have been coated with boehmite gel and fired to 1200°C. The gel-derived alpha alumina crystallized with a strong preferred crystallographic orientation induced by the single crystal proving the solid state epitaxy phenomenon.

31 OCT 1989

CRYSTALLIZATION OF NANOCOMPOSITE GLASSES MADE BY THE SSG PROCESS

FINAL REPORT

to

AIR FORCE OFFICE OF SCIENTIFIC RESEARCH
Bolling Air Force Base, DC 20332

Contract F49620-88-C-0134

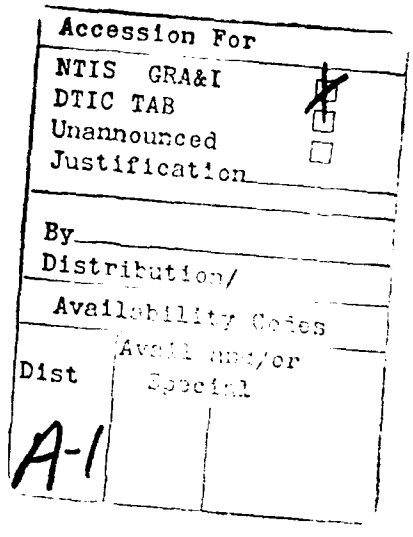

Period Covered:

September 1, 1988 - August 31, 1989

Submitted by

Rustum Roy and Sridhar Komarneni
Materials Research Laboratory
The Pennsylvania State University
University Park, PA 16802

TABLE OF CONTENTS

ABSTRACT

The present research builds in two different directions on the major discovery made under the AFOSR support of the phenomenon of solid state epitaxy. The first goal of the current research is to explore the role of solid state epitaxy in the crystallization of a very much wider range of glass compositions to make glass ceramics. The nanocomposite xerogel route is being utilized to attempt to make a universal glass-ceramic with controllable crystallization. Isostructural seeding of cordierite glass led to a lowering in crystallization temperature due to epitaxy just as in the nucleated crystallization of ceramics. Experiments with other systems such as $LiAlSiO_4$ and $LiAlSi_2O_6$ are in progress and preliminary results show that solid state epitaxy is lowering the crystallization temperatures. The second area of current research is to extend the validity of solid state epitaxy proven by the growth of alumina films on alpha Al_2O_3 single crystals is being extended to other oxides, metals and semiconductors. Epitaxial crystallization of silicon (oxy)carbide glasses such as Nicalon compositions is being investigated in addition to the oxide glasses and gels.

SUMMARY OF PROGRESS

In the last several years with AFOSR support, a very significant advance has been made in breaking really new ground in the exploitation of the sol-gel route for the processing of ceramics. This was the concept of compositional and structural heterogeneity on a nanometer scale in xerogels. The impact is not only evidenced by the list of our own publications, but in the number of papers (e.g. at the Ultrastructure Conference in Tucson) from all over the world which now have started to work on inhomogeneous (nanocomposite) gels. Our invention of the concept and the reality of nanocomposites made via the diphasic and multiphasic gels route is attributable to AFOSR support. The extent of the progress made in the last year of this contract can be gauged by the summary of work accomplished which is given below.

During this year we have prepared diphasic xerogels (or nanocomposite glasses) with isostructural and non-isostructural seeds (with respect to the final phase) in several systems to determine the role of solid state epitaxy in the crystallization of glasses to make glass ceramics. The differences can be traced by comparing two sets of mixtures: (a) glass + very fine crystals of the equilibrium phase and (b) glass + very fine crystals of second (or more) phases with no structural relation to the equilibrium phases.

In order to try to establish the epitaxial nature of the reaction more clearly we have just started to work with single crystal substrates of ceramics, semiconductors and metals.

1. NUCLEATED CRYSTALLIZATION OF OXIDE GLASSES AND GELS

(Structurally and Compositionally Diphasic)

MgO-SiO_2-Al_2O_3 System. The possible role of solid state epitaxy in the crystallization of "nanocomposite cordierite" glass to glass ceramic has been investigated. The use of isostructural (α-cordierite) seeds mixed into cordierite glass led to a lowering in the crystallization temperature to glass ceramic by about 50°C compared to the unseeded glass and gave a very fine microstructure characteristic of glass-ceramics. The use of non-isostructural seeds such as ZrO_2 and TiO_2 did not lower the crystallization temperature of cordierite glass to glass ceramic and in fact in the case of the TiO_2 seeded glass the crystallization temperature increased by about 50°C compared to the

unseeded-cordierite glass. Thus the lowering in crystallization temperature by α-cordierite seeding can be attributed to the epitaxial growth mechanism (see manuscript #1).

The applications of cordierite as a ceramic material are limited by relatively poor mechanical properties which directly result from the inability to sinter cordierite well. Yet the inclusion of α-cordierite seed particles when preparing the gels was not effective in increasing the final density of the material but was successful in lowering the crystallization temperature of α-cordierite. This should not be confused with the compositional heterogeneity (use of diphasic or triphasic gels at the same net 2:2:5 composition) which strikingly increase densification. Lower processing temperatures may extend the uses of cordierite particularly in the electronics industry where multilayered substrates are cofired with low melting metallic conductors. Adding seeds lowered the processing temperature at which the transformation to single phase α-cordierite was complete by as much as 150°C (see manuscript #2).

Silica Glass. Structurally diphasic gels of SiO_2 were prepared using cabosil (ultrafine "glassy" SiO_2 powder) and crystalline seeds of cristobalite (equilibrium phase) or quartz (metastable phase) and heated at 900°, 950°, 1000°, 1100° and 1175°C for several hours to days. The phases present after heat treatments were determined by powder x-ray diffraction. Results to date do not show any significant effect on the crystallization of silica glass by the addition of seeds. Further studies are continuing to confirm these results. This is understandable, since the kinetics of crystallization in SiO_2, are so slow that any nucleation benefit is masked.

Li_2O-SiO_2-Al_2O_3 System. Both structurally and compositionally multiphasic gels are being prepared to see the effects of both isostructural and non-isostructural seeds such as $LiAlSiO_4$, $LiAlSi_2O_6$, α-Al_2O_3, cristobalite or spinel on the crystallization of gels and glasses in order to determine the potential of utilizing solid-state epitaxy or chemical reactions for forming glass ceramics. Results to date have shown that isostructural seeding in gels led to a lowering in crystallization temperature by about as much as 100°C and the use of triphasic (nanocomposite) gels led to enhanced densification.

Na_2O-Al_2O_3-SiO_2 System. Both structurally and compositionally multiphasic gels of albite ($Na_2O.Al_2O_3.6SiO_2$) glass composition were prepared with 5% and 10% α-Al_2O_3, 20% γ-Al_2O_3,

2% and 25% SiO_2 (quartz) or 5% and 20% nepheline seeds. Albite is notoriously slow to crystallize, and the object here was to induce metastable paths to crystallization. Studies with albite seeds are in progress. Results of these experiments showed that nepheline seeds enhanced the crystallization of nepheline phase in this glass and led to a mechanically strong glass ceramic.

SiO_2-B_2O_3-Na_2O-Al_2O_3 Glass. This glass composition is the same as that of Corning 7740 and consists of 81% SiO_2, 13% B_2O_3, 4% Na_2O and 2% Al_2O_3 by weight. Structurally and compositionally multiphasic gels were made with α-Al_2O_3 or quartz seeds and their crystallization behavior studied. Results to date did not show any significant effects of these seeds in this glass composition.

MgO-SiO_2 System. Diphasic gels which are compositionally different resulted in enhanced densification compared to the single phase gels. This result is consistent with earlier results of SiO_2-Al_2O_3 and SiO_2-Al_2O_3-MgO systems (see manuscript #3). Our goal is to see the difference in crystallization of $MgSiO_3$; $MgSiO_3$ + $MgSiO_3$; $MgSiO_3$ + Mg_2SiO_4 seeds in addition to densification.

2. DIRECT VERIFICATION OF SOLID STATE EPITAXY

While many of our previous papers have conclusively demonstrated the epitaxial crystallization from solid xerogels the phenomenon of epitaxy in the solid state is so unusual that a more direct approach to understanding it is justified. In an attempt to prove the validity of the solid-state epitaxy, single crystals and polycrystalline substrates of alumina have been coated with boehmite gel and fired to 1200°C in order to determine whether the gel-derived α-alumina crystallizes with a strong preferred crystallographic orientation induced by the single crystal. On the single crystal, the boehmite gel crystallized in the form of needles on the surface with the same orientation definitely showing some epitaxial control. On the polycrystalline alumina the boehmite gel resulted in an equiaxed grain morpholog quitey unlike that on the single crystal. Experiments with other single crystals such as TiO_2, $SrTiO_3$, Si and Ni are in progress.

3. CATALYZED CRYSTALLIZATION OF NON-OXIDE GLASSES

In addition to oxide glasses, non-oxide glasses have been studied as hosts for catalyzed crystallization. It has been shown that x-ray amorphous glasses--containing up to 18%

carbon--can be synthesized using a sol/gel process. Most importantly, though, Si-C bonds are found in the glasses prepared by heat-treating the gels at high temperature in an inert atmosphere; i.e., the synthesis does, in fact, create an *oxycarbide* structure.

^{1}H NMR, ^{13}C NMR and TGA revealed that the methoxy groups in methy, ethyl, propyl and phenyl trimethoxysilanes are hydrolyzed in the solutions, and therefore, absent in the gels. But the alkyl groups are retained in the dry gels. The ^{29}Si NMR data verified that the Si-C bonds associated with these alkyl groups are intact in the dry gels.

The amount of carbon in the gel is dependent upon the carbon content of the alkyl group in the precursor, but the carbon content in the glass is limited to 12-18%. Thus, it is proposed that only the carbon atom bonded directly to the silicon can be retained in the glass structure. The other carbon atoms in the alkyl chain of the gel probably react with hydroxyl and silicate species to evolve CO and CO_2 and/or to precipitate amorphous carbon second phase particles. Of course, the reactions must be more complex than this because some fraction of the Si species in the glass were found to have two carbon ligands. Until the bonding and cross-linking of these carbon ligands in the glass are fully characterized, this issue will be uncertain. Nevertheless, these data suggest that the methyl-trimethoxysilane is the most appropriate oxy-carbide glass precursor unless excess amorphous carbon (second-phase) is desired in the microstructure. The ^{13}C NMR did suggest the presence of amorphous carbon in the glasses, but its concentration, distribution and effect upon the glass properties has not yet been determined.

The TGA analyses of the glasses--in air--revealed that these materials are oxidation resistant to 1000°C. The oxidation of SiC occurs in the range 500°-1000°C, and this provides a sense of thermodynamic stability to the glass. And since oxygen must diffuse through the glass to oxidize the Si-C bonds, a measure of kinetic stability is also provided. Studies are now in progress to attempt to find effects of silicon carbide seeding on these gel-derived oxycarbide glasses (see manuscript #4).

CUMULATIVE LIST OF PUBLICATIONS AND PRESENTATIONS

SUPPORTED BY AFOSR

1. D. Hoffmann, R. Roy and S. Komarneni, "Diphasic Ceramic Composites via a Sol-Gel Method," Mat. Letters 2, 245-247 (1984).
2. D. Hoffmann, S. Komarneni and R. Roy, "Preparation of a Diphasic Photosensitive Xerogel," J. Mat. Sci. Letter 3, 439-442 (1984).
3. R. Roy, S. Komarneni and D.M. Roy, "Multiphasic Ceramic Composites Made by Sol-Gel Technique," in the Proceedings of the Symposium on "Better Ceramics Through Chemistry" (Eds. C.J. Brinker et al.), Elsevier, North-Holland, pp. 347-359 (1984) (jointly supported by NSF).
4. D.W. Hoffmann, R. Roy and S. Komarneni, "New Sol-Gel Strategies for Making Ceramic-Ceramic Composites," Abstracts, 1984 American Ceramic Society Meeting, Am. Ceram. Soc. Bull. 63, 459 (1984).
5. R. Roy, S. Komarneni and D.W. Hoffmann, "Sol-Gel Approach to Making Photochromic Xerogels and Glasses," Abstracts, 1984 American Ceramic Society Meeting, Am. Ceram. Soc. Bull. 63, 499 (1984).
6. R. Roy, L.J. Yang and S. Komarneni, "Controlled Microwave Sintering and Melting of Gels," Abstracts, 1984 American Ceramic Society Meeting, Am. Ceram. Soc. Bull. 63, 459 (1984).
7. S. Komarneni, L.J. Yang and R. Roy, "Hydrothermal Reaction Sintering of Single and Diphasic Xerogels," Abstracts, 1984 American Ceramic Society Meeting, Am. Ceram. Soc. Bull. 63, 459 (1984).
8. R. Roy, S. Komarneni and L.J. Yang, "Controlled Microwave Sintering and Melting of Gels," J. Am. Ceram. Soc. 68, 392 (1985).
9. S. Komarneni, R. Roy, E. Breval and Y. Suwa, "Hydrothermal Route to Ultrafine Powders Utilizing Single and Diphasic Gels," Abstracts of the Second International Symposium on Hydrothermal Reactions in University Park, p. 62.

10. S. Komarneni, R. Roy, E. Breval, M. Ollinen and Y. Suwa, "Hydrothermal Route to Ultrafine Powders Utilizing Single and Diphasic Gels," Adv. Ceramic Mats. 1, 87 (1986).

11. R. Roy, Y. Suwa and S. Komarneni, "Nucleation and Epitaxial Growth in Reactions of the Diphasic (Crystalline + Amorphous) Gels," presented at the Second International Conference on Ultrastructure Processing of Ceramics, Glasses and Composites in February 1985 (jointly supported by NSF).

12. T.C. Simonton and R. Roy, "Natural Gel Derived Ceramics: Chemistry, Microstructure and Properties of Opal, Chert, Agate, Etc.," Abstracts of the American Ceramic Society Meeting, Cincinnati, OH, 1985, p. 269.

13. R. Roy, "Seeding: A Special Approach to Diphasic Xerogels," Abstracts of the American Ceramic Society Meeting, Cincinnati, OH, 1985, p. 270.

14. R. Roy, "Microwave Melting of Ceramics and Gels," Patent applications filed via AFOSR.

15. C. Scherer and C. Pantano, "Ti-Si Glasses Using a Colloidal Sol-Gel Process," presented at the Third International Workshop on Glasses and Glass Ceramics from Gels, Montpellier, France, 1985.

16. S. Komarneni and R. Roy, "Microwave Processing of Zeolites," AF Invention 17310 (1985).

17. Y. Suwa, R. Roy and S. Komarneni, "Crystallographic Effects in Seeded (Diphasic Gels): II. Microstructural and Sintering Properties," Abstracts of the American Ceramic Society Meeting, Cincinnati, OH, 1985, p. 270.

18. Y. Suwa, R. Roy and S. Komarneni, "Enhancing Densification by Solid State Epitaxy in Structurally Diphasic Al_2O_3-MgO Xerogels," Abstracts, Materials Research Society, 1985 Fall Meeting, p. 468 (1985).

19. S. Komarneni and R. Roy, "Anomalous Microwave Sintering and Melting of Zeolites," Abstracts, Materials Research Society, 1985 Fall Meeting, p. 468 (1985).

20. R. Roy, Y. Suwa and S. Komarneni, "Nucleation and Epitaxial Growth in Reactions of Diphasic (Crystalline + Amorphous) Gels," in Ultrastructure Processing of Ceramics, Glasses and Composites (Eds. L.L. Hench and D.R. Ulrich), pp. 247-258 (1986).

21. Y. Suwa, R. Roy and S. Komarneni, "Lowering Sintering Temperature and Enhancing Densification by Epitaxy in Structurally Diphasic Al_2O_3 and Al_2O_3-MgO Xerogels," Mat. Sci. Eng. 83, 151 (1986).

22. S. Komarneni and R. Roy, "Anomalous Microwave Melting of Zeolites," Mat. Lett. 4, 107 (1986).

23. S. Komarneni, G. Vilmin, Y. Suwa and R. Roy, "Enhancing Densification of Al_2O_3-MgO Xerogels by Double Seeding with α-Al_2O_3 and $MgAl_2O_4$," Abstracts. The American Ceramic Society 88th Annual Meeting, p. 92 (1986).

24. S. Komarneni, A. Kijowski, T.C. Simonton and R. Roy, "Diphasic Glass Composites," Abstracts, The American Ceramic Society 88th Annual Meeting, p. 92 (1986).

25. T.C. Simonton, S. Komarneni and R. Roy, "Diphasic Composites of Natural Gel Derived Ceramics," Abstracts, The American Ceramic Society 88th Annual Meeting, p. 117 (1986).

26. T.C. Simonton, S. Komarneni and R. Roy, "Radiation Assisted Chemical Bonding of Natural and Synthetic Gel-Derived Ceramics," Abstracts, The American Ceramic Society 88th Annual Meeting, p. 122 (1986).

27. S. Komarneni, Y. Suwa and R. Roy, "Application of Compositionally Diphasic Xerogels for Enhanced Densification: The System Al_2O_3-SiO_2," J. Am. Ceram. Soc. 69, C-155 (1986).

28. T.C. Simonton, R. Roy, S. Komarneni and E. Breval, "Microstructure and Mechanical Properties of Synthetic Opal: A Chemically Bonded Ceramic," J. Mat. Res. 1, 667 (1986).

29. S. Komarneni, Y. Suwa and R. Roy, "Enhancing Densification of 93% Al_2O_3-7% MgO Triphasic Xerogels with Crystalline α-Al_2O_3 and $MgAl_2O_4$ Seeds," J. Mat. Sci. Lett. 6, 525 (1987).

30. T.C. Simonton, S. Komarneni and R. Roy, "Ultrafine Microstructure in Synthetic Opal, A Diphasic Composite," Abstracts, Materials Research Society, 1986 Fall Meeting, p. 747 (1986).

31. W.A. Yarbrough and R. Roy, "Extraordinary Effects of Mortar-and-Pestle Grinding on Microstructure of Sintered Alumina Gel," Nature 322, 347 (1986).

32. C.P. Scherer and C.G. Pantano, "Titania-Silica Glasses Using a Colloidal Sol-Gel Process," J. Non-Cryst. Solids 82, 246 (1986).

33. W.A. Yarbrough and R. Roy, "Microstructure Evolution in Sintering of AlOOH Gels," J. Mat. Res. (in press).

34. R. Roy, "Some New Advances with SSG Derived Nanocomposites," Abstracts, Third International Conference on Ultrastructure processing of Ceramics, Glasses and Composites, p. 44 (1987).

35. R. Roy, S. Komarneni and W.A. Yarbrough," Some New Advances with SSG Derived Nanocomposites," Third International Conference on Ultrastructure Processing of Ceramics, Glasses and Composites (Eds. J.D. MacKenzie and D.R. Ulrich) (submitted for publication).

36. D. Zaide, E. Breval and C.G. Pantano, "Colloidal Sol/Gel Processing of Ultra-low Expansion TiO_2/SiO_2 Glasses," presented at the Fourth International Workshop on Glasses-Ceramics from Gels, Kyoto, Japan, 1987.

37. Y. Suwa, S. Komarneni and R. Roy, "Effect of Seeding on Crystallization and Sintering of Diphasic Al_2O_3-MgO Monolithic Gels," Proceedings of the Japanese Ceramic Society, Vol. 3, pp. 735-736 (1987).

38. Y. Suwa, R. Roy and S. Komarneni, "Effect of Epitaxial Seeding on Crystallization Process and on Densification in Diphasic Al_2O_3-MgO Xerogel," Abstracts, '87 International Symposium & Exhibition on Science and Technology of Sintering, Tokyo, Japan, p. 420-421 (1987). (Also, in press.)

39. S. Komarneni, "Hydrothermal Preparation of Low-Expansion 'NZP' Family of Materials," '87 International Symposium & Exhibition on Science and Technology of Sintering, Tokyo, Japan, p. 422 (1987). (Also, in press.)

40. R. Roy, "The Al_2O_3-SiO_2 Phase Diagram: Metastability and Order-Disorder," Abstracts, 1st International Workshop on Mullite, p. 13 (1987); and submitted for publication.

41. S. Komarneni and R. Roy, "Mullite Derived From Diphasic Gels," Abstracts, 1st International Workshop on Mullite, p. 23 (1987); and submitted for publication.

42. R. Roy, "Ceramics Via the Solution-Sol-Gel Route," Science 238, 1664-1669 (1987).

1988-1989

43. A.K. Kijowski, S. Komarneni and R. Roy, "Multi-phasic Nanocomposite Sol-Gel Processing of Cordierite," Better Ceramics Through Chemistry, Vol. III (C.J. Brinker, D.E. Clark and D.R. Ulrich, eds.), Mat. Res. Soc. Proc., Pittsburgh, PA, pp. 245-250 (1988).

44. S. Komarneni, E. Breval and R. Roy, "Microwave Preparation of Mullite Powders," Abstracts, Materials Research Society Spring Meeting, Reno, Nevada (1988).

45. S. Komarneni, E. Breval and R. Roy, "Microwave Preparation of Mullite Powders," in Microwave Processing of Materials (M.H. Brooks, I.J. Chabinsky and W.H. Sutton, eds.). Mat. Res. Soc. Proc., Pittsburgh, PA, pp. 235-238 (1988).

46. S. Komarneni, "Nanocomposite Sol-Gel Processing," New Ceramics (invited paper in Japanese) 2, 89-94 (1989).

47. H. Zhang and C.G. Pantano, "Sol-Gel Processing of Si-O-C Glasses for Glass Matrix Composites," Ultra Structure Processing of Advanced Ceramics (submitted).

48. A.M. Kazakos, S. Komarneni and R. Roy, "Sol-Gel Processing of Cordierite: Effect of Seeding and Optimization of Heat Treatment," J. Mat. Res. (submitted).

49. A.M. Kazakos, "Sol-Gel Processing of Cordierite," M.S. Thesis, Graduate School, The Pennsylvania State University, pp. 115 (1989).

50. R. Roy, "Synthesizing New Materials to Specification," Solid State Ionics 32/33, 3-22 (1989).

MANUSCRIPT #1

Seeding Effects on Crystallization Temperatures of Cordierite Glass Powder

SEEDING EFFECTS ON CRYSTALLIZATION TEMPERATURES OF CORDIERITE GLASS POWDER

U. Selvaraj, S. Komarneni and R. Roy
Materials Research Laboratory
The Pennsylvania State University
University Park, PA 16802

ABSTRACT

The role of solid state epitaxy in the crystallization of nanocomposite cordierite glass to glass ceramic was investigated. The use of isostructural (α-cordierite) seeds in cordierite glass led to a lowering in the crystallization temperature to form glass ceramic by about 50°C compared to the unseeded glass. The use of non-isostructural seeds such as ZrO_2 and TiO_2 did not lower the crystallization temperature of cordierite glass to glass ceramic and in fact in the case of the TiO_2 seeded glass the crystallization temperature increased by about 50°C compared to the unseeded α-cordierite glass. The lowering in crystallization temperature by α-cordierite seeding can be attributed to the nucleation and epitaxial growth mechanism.

INTRODUCTION

The well-known technology of the production of bulk glass-ceramic articles of varying sizes is based on the controlled crystallization of glasses between their glass transition temperatures and melting points.[1-3] Often a few percent of oxides such as TiO_2, ZrO_2 and P_2O_5 are added to these glass-forming systems.[2] This results in glass ceramics with a large number of fine crystals, which is attributed to the heterogeneous nucleating characteristic of these oxides though they do not appear in the nucleating step. Roy[4] proposed a radically different explanation; that is, metastable liquid immiscibility as the cause of very fine segregation and fine structured crystallization in all such systems which was experimentally confirmed by Porai-Koshits and his coworkers.[5] In recent years Roy et al.[6-8] in this laboratory have studied the effects of seeds in monophasic and multiphasic gel powders, which provided unambiguous evidence for the use of isostructural foreign crystalline nuclei as the basis for fine microstructure crystallization of amorphous solids. It was shown that multiphasic xerogels enhanced densification of ceramics and introduction of epitaxial substrate or seed accelerated the kinetics of formation of thermodynamically stable solid phase because epitaxial seeds catalyze the growth of a phase by providing a large number of nuclei with the structure of the desired phase. The epitaxial crystallization has been clearly demonstrated in $ThSiO_4$ gels[9] seeded with either huttonite or thorite.

The effect of isostructural and non-isostructural seeds on glass crystallization, however, has not been investigated thus far. The manufacture of glass ceramics, by sintering of glass powder, is suitable for the production of small quantities of articles of complicated shapes such as heat exchangers.[10] For instance, if these glasses crystallize from their surface, as in cordierite glass powder, the significant surface area of glass powder ensures very fine structured crystallization. Seeding by the crystals of the final equilibrium phase or others may help to enhance or regulate the process.

In oder to determine the role of nucleation and epitaxial growth in nanocomposite glasses a study of seeding effects on cordierite glass powder was undertaken. Seeds such as α-cordierite, ZrO_2 and TiO_2 were added to the glass powder and the phase transformation mechanism was monitored by Differential Thermal Analysis (DTA) and X-ray Diffraction (XRD).

EXPERIMENTAL PROCEDURE

Preparation of Bulk Cordierite Glass and Fine Powder

Bulk cordierite glass was prepared from monophasic cordierite gel; the gel preparation was discussed in detail elsewhere.[13] Cordierite gel was taken in a 50 ml platinum crucible and heated at 350° and 700°C to decompose organics and nitrates respectively. The decomposed material was transferred to a molybdenum disilicide furnace which was kept at 1200°C. The temperature was then increased to 1600°C and maintained at this temperature for 12 hrs. The glass melt in the platinum crucible was removed from the furnace and was shaken occasionally to remove the bubbles and to obtain better homogeneity. Homogeneous cordierite glass rods were formed by pouring the melt in brass moulds, kept at room temperature. The cordierite glass was powdered and sieved through -325 mesh. Fine powders were produced by further grinding in a Spex mixer/mill using methacrylate balls. These powders were then suspended in alcohol and the suspension was collected and dried to obtain fine glass particles.

Preparation of Seeds

α-cordierite was prepared by heating cordierite gel to 1300°C for 12 hrs. The crystalline material was powdered using an agate mortar and pestle. The powder was suspended in water for several hours to yield an agglomerate-free suspension of fine seed particles (0.05-0.5 μm). Hydrothermally prepared tetragonal ZrO_2 seeds (50-80 nm) were obtained from Chichibu Cement Co., Ltd. Anatase seeds (60-100 nm) were prepared by heating TiO_2 gel suspended in water (5 g of gel in 100 ml of water) in a Parr bomb at 150°C for 3 days. The particle sizes of different seeds were determined using a Phillips 420 transmission electron microscope.

Seeded glass powders were made by thoroughly mixing the powders and appropriate quantities of seeds in alcohol using an agate mortar and pestle. The thermal reactions of the seeded and unseeded glasses were studied by a Perkin Elmer (Model DTA 1700) differential thermalanalyser. X-ray diffraction of powder samples heated at various temperatures was carried out using a Scintag USA Pad-V diffractometer with Ni filtered CuKα radiation. The relative intensity of α-cordierite (100) peak, expressed in arbitrary units, was obtained by comparing the area of the α-cordierite (100) peak and that of a standard [quartz (100) peak]. The area of these peaks were calculated by collecting the XRD data at 0.1° 2θ/min. and integrating these data points using the area program of the Scintag (XDS) Fortran IV software package.

RESULTS AND DISCUSSION

Differential Thermaly Analyses

Figure 1 shows the DTA curves generated when bulk cordierite glass and cordierite glass powder without seed and with seeds such as α-cordierite, TiO_2 and ZrO_2 are heated at 10°C/min. The less predominant endothermic shifts observed between 820° and 840°C in all the cases are associated with the glass transition temperature of cordierite glass. On further heating, in contrast, prominent features such as two characteristic exothermic peaks were observed (Fig. 1) which are attributed to the formation of μ-cordierite at about 940°C and α-cordierite at about 1000°C based on the following XRD experimental data. These results are consistent with those reported by several workers.[13-15] In prticular, the XRD data of Mussler and Shafer[13] indicated that cordierite glass powder started crystallizing at about 880°C while α-cordierite began forming around 1000°C which attained a maximum value at 1046°C. For the bulk glass (Fig. 1a), the two overlapped crystallization exotherms are seen at 1075° and 1095°C which are shifted towards lower temperatures for finely ground glass powder (Fig. 2b). This may be explained by the known surface crystallization mechanism of cordierite glass. Furthermore, in the latter case, the peaks are well separated, that is the temperature difference between the crystallization exotherm, T_{cr}, is large because in the lower temperature regime longer temperature interval is necessary for attainment of the maximum heat of crystallization of α-cordierite. Figures 1c, 1d and 3e show the DTA curves for cordierite glass powder seeded with 5 wt% α-cordierite, ZrO_2 and TiO_2 respectively. Addition of seed did not seem to affect the maximum in the crystallization temperature of μ-cordierite while the μ-cordierite to α-cordierite transformation temperature decreased for cordierite glass powder seeded with α-cordierite. On the contrary, the transformation temperature increased slightly for cordierite glass powder seeded with ZrO_2 and TiO_2 (Fig. 1). Similar effects have been observed in a number of gels seeded with isostructural and non-isostructural seeds.[6-8] The magnitude of lowering in crystallization temperature by isostructural seeding in glasses found here is

markedly lower than that in gels.[6] The isostructural and non-isostructural seeding effects became quite clear when these seeded glass pellets were sintered at various temperatures for longer times and the crystallization mechanism was followed by X-ray diffraction.

X-Ray Diffraction Analyses

Figure 2 shows the X-ray diffraction patterns for glass seeded with 5 wt% α-cordierite, calcined at 875°C for different lengths of time. It can be seen from Figure 2 that μ-cordierite transformed completely to α-cordierite within approximately 40 hours at 875°C. However, under similar conditions glass seeded with 5 wt% TiO_2 and ZrO_2 exhibited no evidence for the formation of α-cordierite, though seeded and unseeded glass powders showed the formation of μ-cordierite when heated at 850°C for 6 hrs while ~5 wt% of α-cordierite was formed in the unseeded glass powder. The transformation of μ-cordierite to α-cordierite is further confirmed by plotting the relative intensity of α-cordierite (100) peak of seeded and unseeded glasses calcined at 875°C for different durations (Fig. 3). The trend in Fig. 3 clearly indicates that isostructural α-cordierite seeds catalyze the transformation of μ-cordierite to α-cordierite by providing nuclei of α-cordierite. As a result, the crystallization temperature of α-cordierite is lowered which presumably is due to solid state epitaxial growth. The lowering of crystallization temperature by seeding is also associated with enhanced densification at lower temperatures for a number of monophasic and multiphasic gels which resulted in lower ceramic processing temperatures. We, therefore, plan to investigate the densification details of these nanocomposite glass materials at a later date.

The phase evolution for seeded and unseeded cordierite glass powders at various temperatures but at a constant heating time of 6 hrs, is depicted in Figures 4-7. These powders remain amorphous up to 830°C. All these glass powders crystallized to μ-cordierite at 850°C, while the unseeded (Fig. 4) and α-cordierite (Fig. 5) and ZrO_2 (Fig. 6) seeded glasses transformed completely to α-cordierite at 925°C. On the contrary, TiO_2 seeded glass powder (Fig. 7) exhibited a definite "negative catalyst effect"; it crystallized to α-cordierite only at 1000°C. The difference in the crystallization temperature of α-cordierite for glasses seeded with TiO_2 and α-cordierite is approximately 100°C. The reason for the "negative catalyst effect" of TiO_2 is not understood. Similar interesting effect has been observed in the crystallization of zircon seeded with α-$ThSiO_4$.[9]

Acknowledgement

This research was supported by U.S. Air Force Office of Scientific Research under Contract No. F49620-88-C-0134.

REFERENCES

(1) S.D. Stookey, J.S. Olcott, H.M. Garfinkel and D.L. Rothermel, "Advances in Glass Technology," Plenum Press, New York (1962), pp. 397.

(2) P.W. McMillan, "Glass-Ceramics," Academic Press, New York (1964).

(3) J.J. Hammel, in "Advances in Nucleation and Crystallization in Glasses," edited by L.L. Hench and S.W. Freiman, The American Ceramic Society, Inc., Columbus, OH (1971), p. 1.

(4) R. Roy, "Metastable Liquid Immiscibility and Subsolidus Nucleation," J. Am. Ceram. Soc. 43, 670 (1960).

(5) E.A. Porai-Koshits, in "Phase Separation of Glasses," edited by O.V. Mazurin and E.A. Porai-Koshits, North Holland (1984), p. 111.

(6) R. Roy, "Ceramics Via the Solution-Sol-Gel Route," Science 238, 1664 (1987).
(7) R. Roy, Y. Suwa and S. Komarneni, in "Science of Ceramic Chemical Processing," edited by L.L. Hench and D.R. Ulrich, John Wiley (1986), p. 247.
(8) R. Roy, S. Komarneni and W.A. Yarbrough, "Some New Advances with SSG-Derived Nanocomposites," Chapter 42, Ultrastructure Processing of Advanced Ceramics, J.D. MacKenzie and D.R. Ulrich (eds.), Wiley Interscience, pp. 571-588 (1988).
(9) G. Vilmin, S. Komarneni and R. Roy, "Crystallization of $ThSiO_4$ from Structurally and/or Compositionally Diphasic Gels," J. Mater. Res. 2, 489 (1987).
(10) D.M. Miller, "Sintered Cordierite Glass-Ceramic Bodies," U.S. Patent 3 926 648, Dec. 16, 1975.
(11) C.I. Helgesson, in "Science of Ceramics," British Ceramic Society, Staffordshire (1976), Vol. 8, p. 347.
(12) A.M. Kazakos, Thesis, The Pennsylvania State University, University Park (1989).
(13) B.H. Mussler and M.W. Shafer, "Preparation and Properties of Mullite-Cordierite Composites," Ceram. Bull. 63, 705 (1984).
(14) G.H. Beall, in "Commercial Glasses," edited by D.C. Boyd and J.F. MacDowell, The American Ceramic Society, Inc., Columbus (1986), Vol. 18, p. 157.
(15) A.G. Gregory, T.J. Veasey, "The Crystallization of Cordierite Glass," J. Mater. Sci. 6, 1312 (1971).

FIGURE CAPTIONS

Figure 1. DTA curves at 10°C/min for cordierite glasses: (a) bulk sample; (b) powder sample; (c) powder seeded with 5 wt% α-cordierite; (d) powder seeded with 5 wt% ZrO_2; and (e) powder seeded with 5 wt% TiO_2.

Figure 2. Powder X-ray diffraction patterns as a function of heat treatment time (hours) for cordierite glass powder seeded with 5 wt% α-cordierite, calcined at 875°C.

Figure 3. Relative intensity of α-cordierite (100) peak in comparison with a standard, quartz (101) peak, heated at 875°C for different times for cordierite glass powder without seed (❑) and with (●) 5 wt% α-cordierite seed.

Figure 4. Powder X-ray diffraction patterns for unseeded cordierite glass powder as a function of temperature at a constant heating time.

Figure 5. Powder X-ray diffraction patterns for 5 wt% α-cordierite seeded cordierite glass powder as a function of temperature at a constant heating time.

Figure 6. Powder X-ray diffraction patterns for 5 wt% ZrO_2 seeded cordierite glass powder as a function of temperature at a constant heating time.

Figure 7. Powder X-ray diffraction patterns for 5 wt% TiO_2 seeded cordierite glass powder as a function of temperature at a constant heating time.

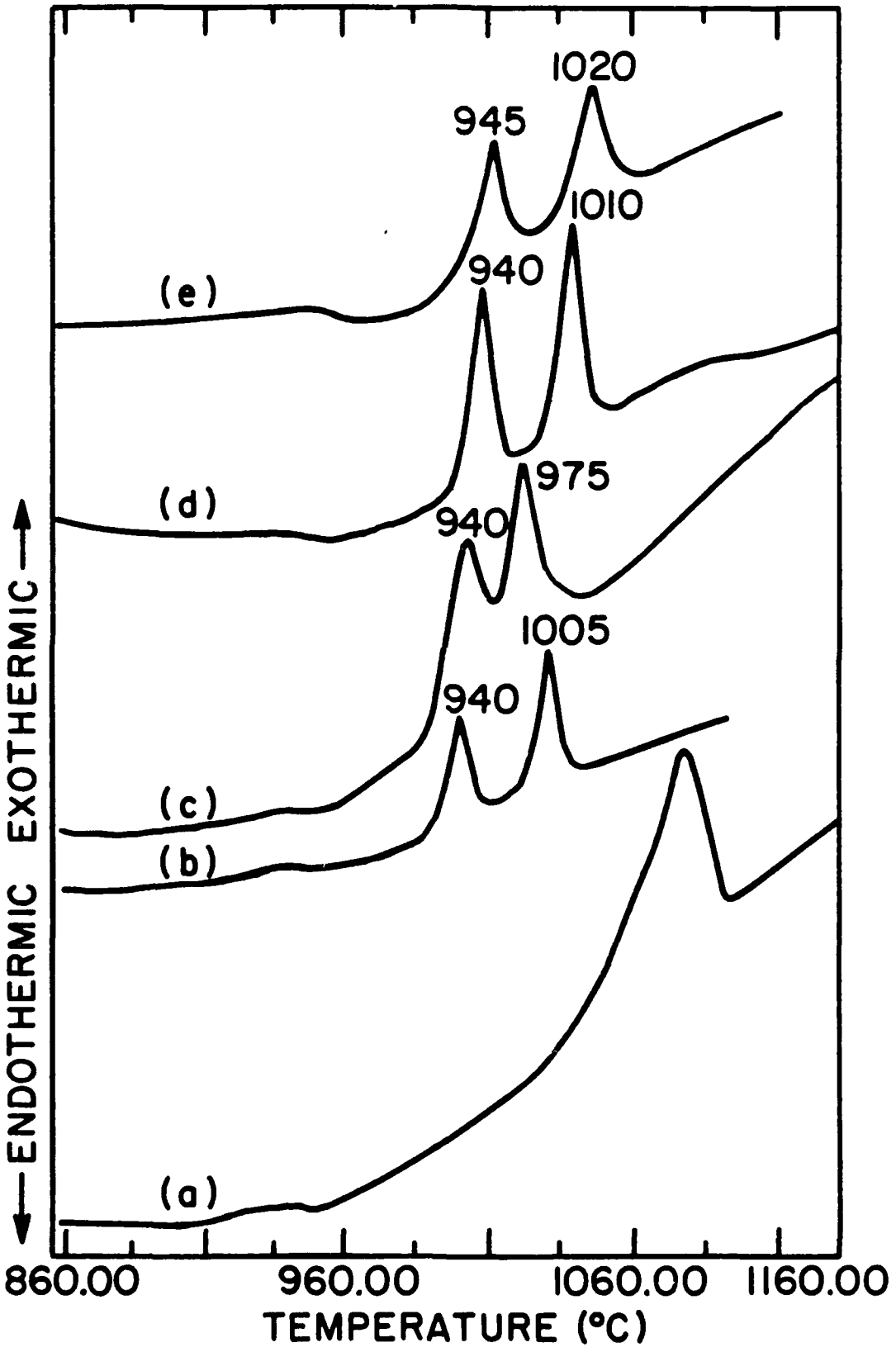
1020
945
1010
940
(e)
(d)
975
940
1005
940
(c)
(b)
(a)
ENDOTHERMIC EXOTHERMIC
860.00
960.00
1060.00
1160.00
TEMPERATURE (°C)

Figure 1.

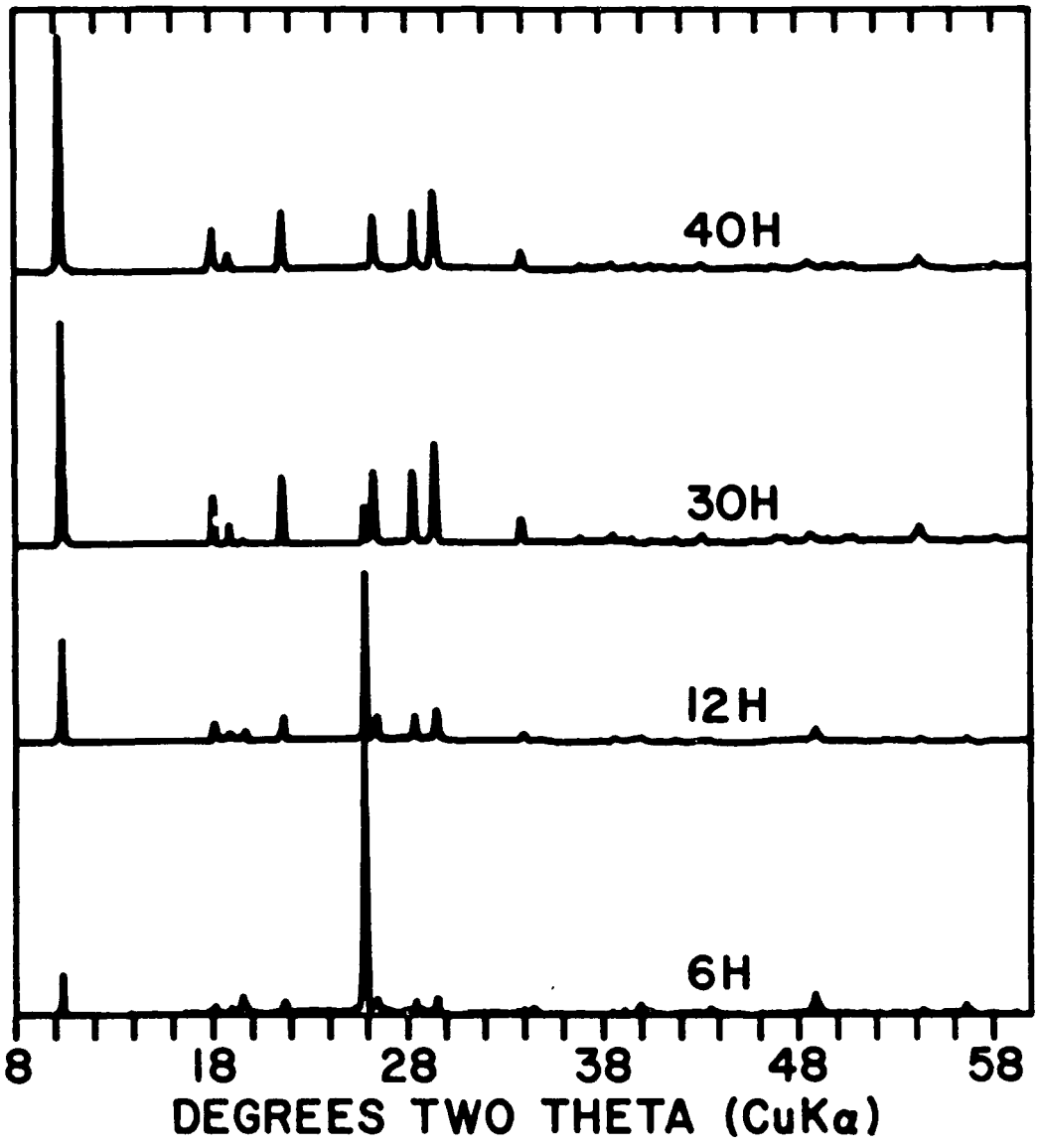

Figure 2.

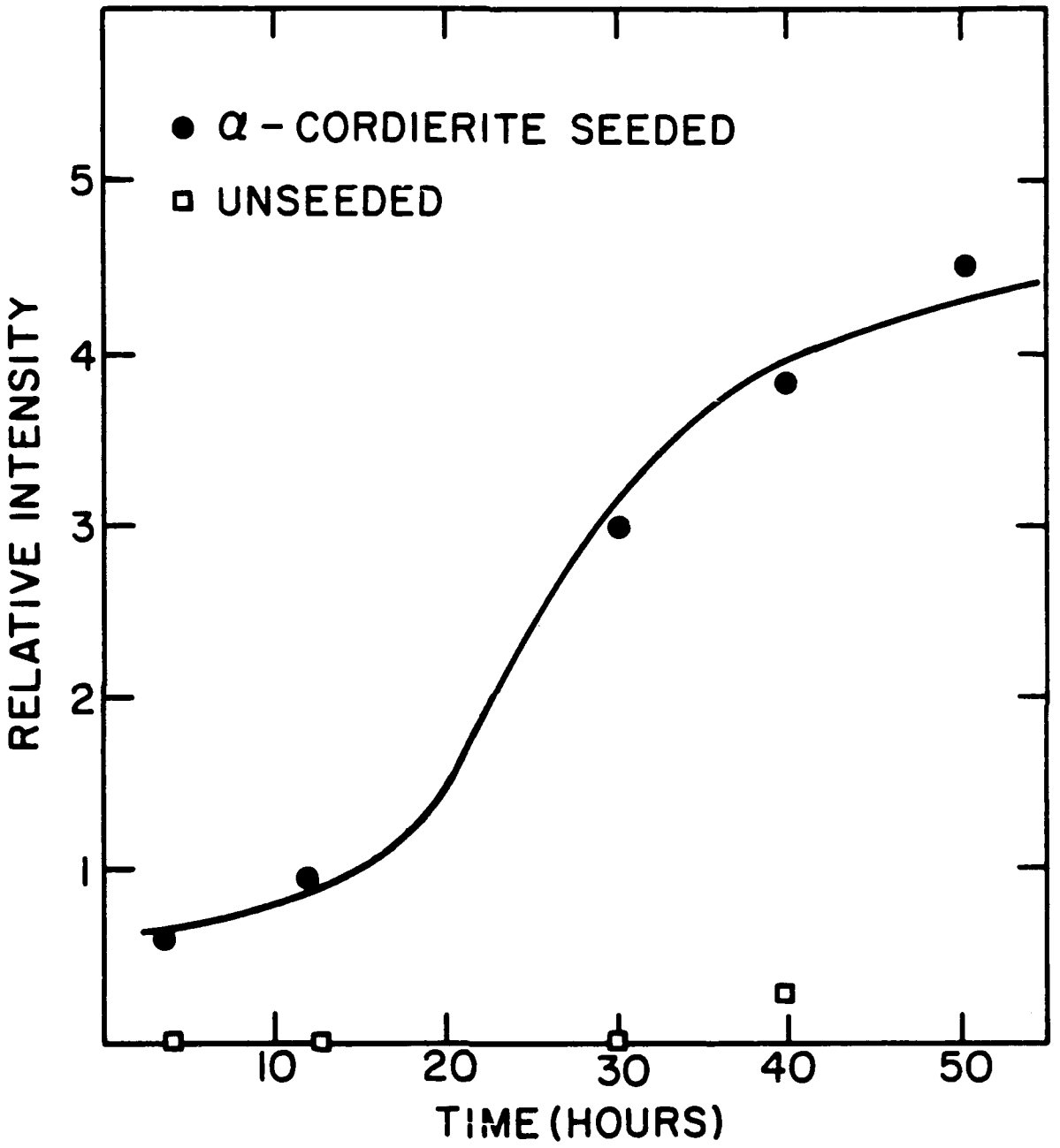
α - CORDIERITE SEEDED
UNSEEDED
RELATIVE INTENSITY
1
2
3
4
5
10
20
30
40
50
TIME (HOURS)

Figure 3.

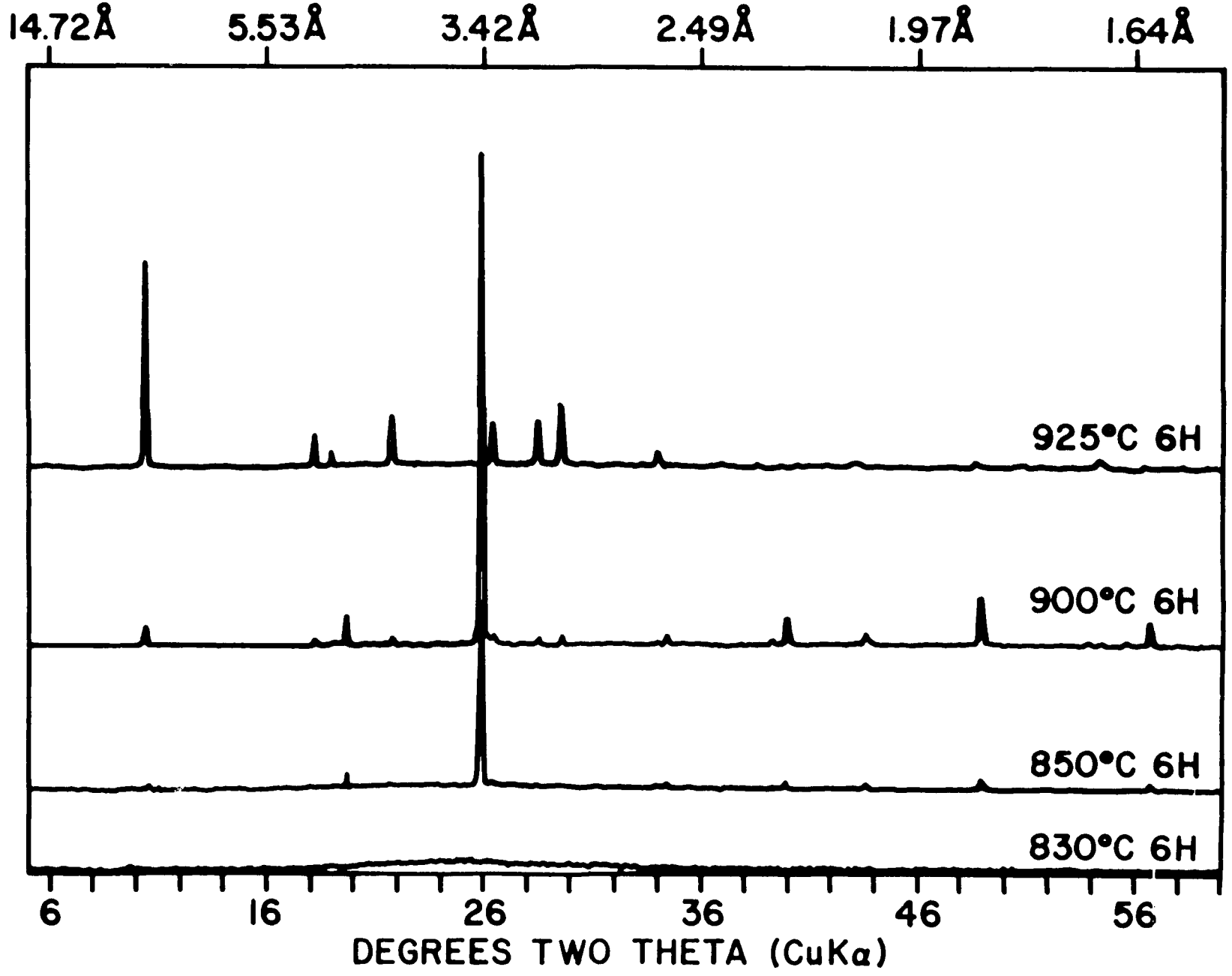
14.72Å
5.53Å
3.42Å
2.49Å
1.97Å
1.64Å
925°C 6H
900°C 6H
850°C 6H
830°C 6H
6
16
26
36
46
56
DEGREES TWO THETA (CuKα)

Figure 4.

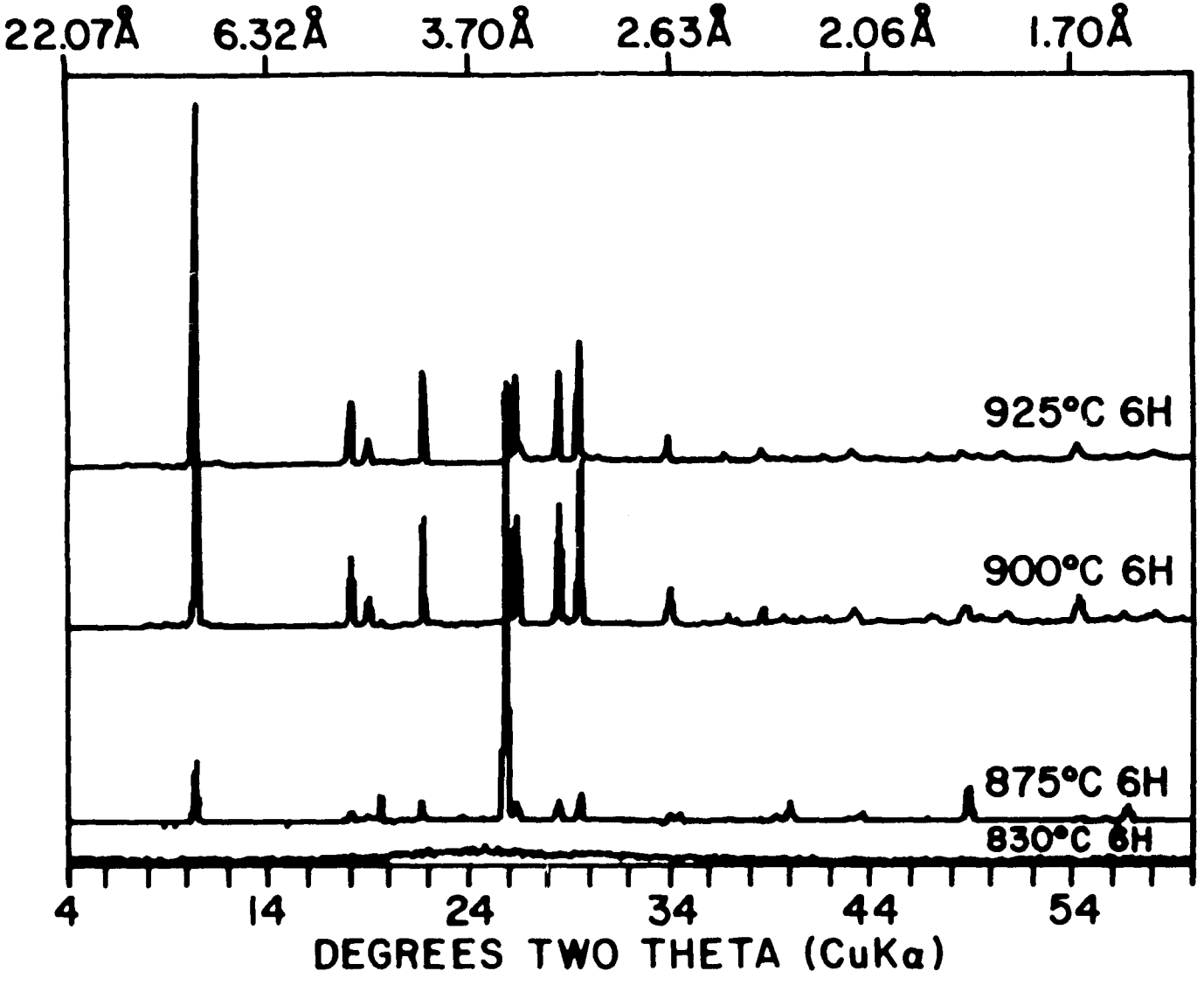
22.07Å
6.32Å
3.70Å
2.63Å
2.06Å
1.70Å
925°C 6H
900°C 6H
875°C 6H
830°C 6H
4
14
24
34
44
54
DEGREES TWO THETA (CuKα)

Figure 5

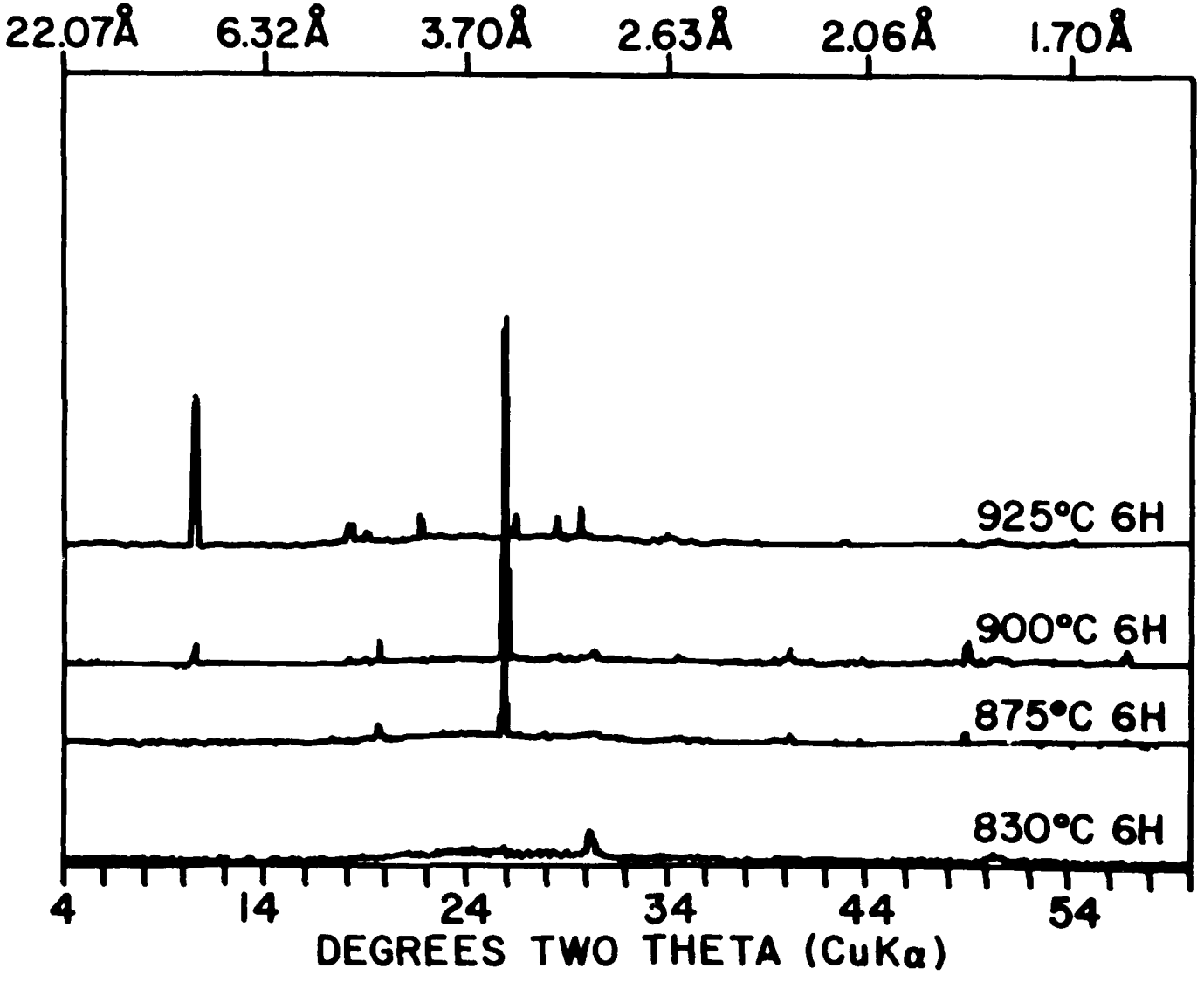
22.07Å
6.32Å
3.70Å
2.63Å
2.06Å
1.70Å
925°C 6H
900°C 6H
875°C 6H
830°C 6H
4
14
24
34
44
54
DEGREES TWO THETA (CuKα)

Figure 6.

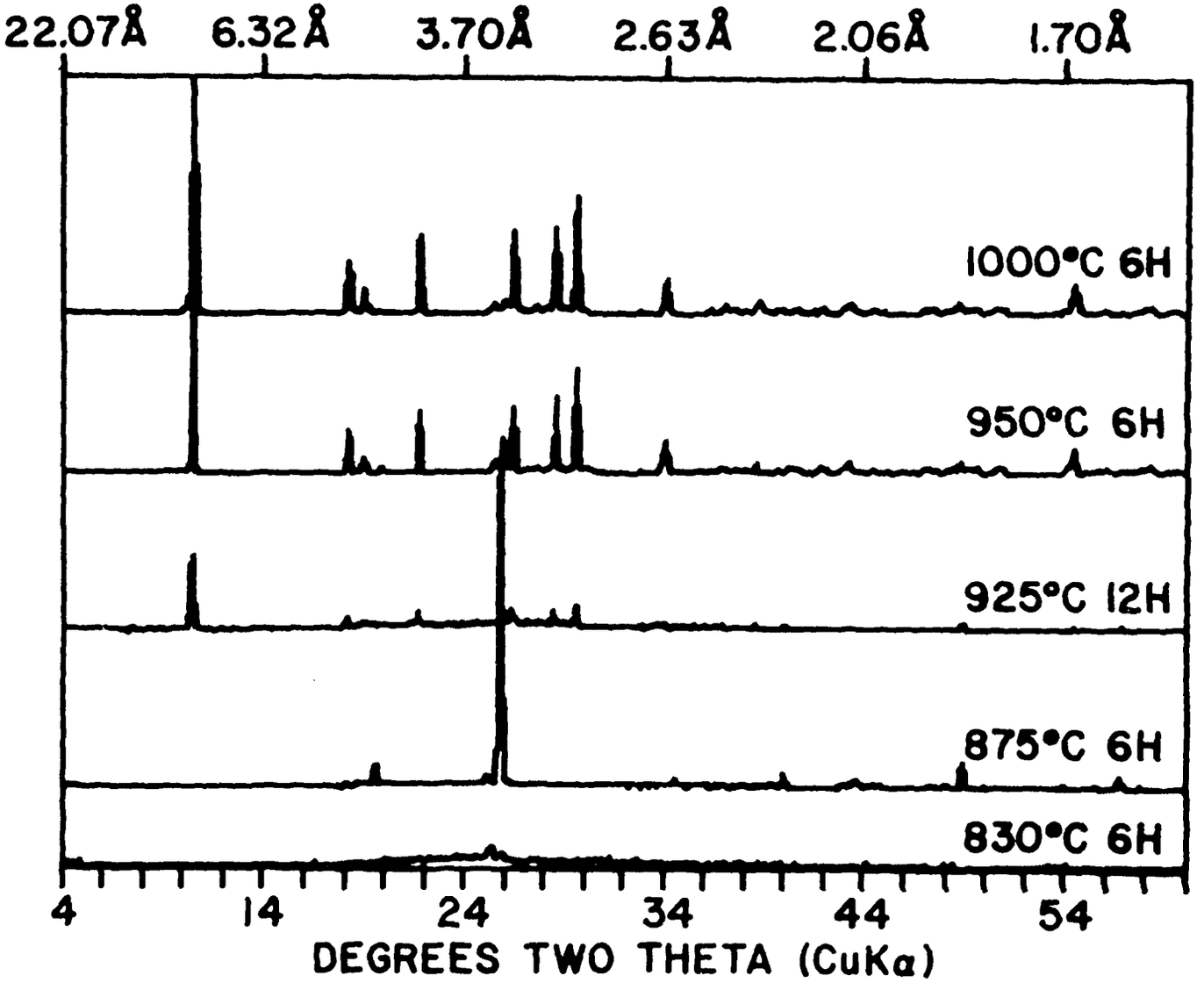
22.07Å
6.32Å
3.70Å
2.63Å
2.06Å
1.70Å
1000°C 6H
950°C 6H
925°C 12H
875°C 6H
830°C 6H
4
14
24
34
44
54
DEGREES TWO THETA (CuKα)

Figure 7.

MANUSCRIPT #2

Sol-Gel Processing of Cordierite:

Effect of Seeding and Optimization of Heat Treatment

ABSTRACT

Three series of cordierite powders were prepared by the sol-gel route; a single phase (monophasic) gel prepared from alkoxides, a nominally triphasic nanocomposite gel made with two nanosized powders and one solution phase, and a truly compositionally triphasic nanocomposite gel prepared from three nanosized powders. Crystalline α-cordierite seeds were also incorporated with the gels and their effectiveness as nucleating agents was investigated and found to lower the crystallization temperature of α-cordierite by 125-150°C. The densification behavior of powder compacts was examined and alterations made to the heat treatment until optimum conditions were found. The truly triphasic compact sintered at 1300°C for 2 hours resulted in 100% of theoretical density whereas the nominally triphasic and monophasic pellets densified to 96% and 80% respectively. The enhanced densification achieved with powder compacts prepared from triphasic nanocomposite gels is due in part to the excess free energy of the three components.

SOL-GEL PROCESSING OF CORDIERITE: EFFECT OF SEEDING AND OPTIMIZATION OF HEAT TREATMENT

Ann M. Kazakos, Sridhar Komarneni, and Rustum Roy
Materials Research Laboratory, The Pennsylvania State University, University Park, Pennsylvania 16802

I. INTRODUCTION

Cordierite as a ceramic material has a wide range of uses and applications stemming from its important properties of low thermal expansion and dielectric constant coupled with high chemical and thermal stability. For example, extruded cordierite honeycomb substrates coated with catalysts have become an intricate part of the catalytic converter system in automobiles withstanding severe temperature and chemical environments [1-3]. Other severe conditions where cordierite ceramics are employed include interior walls of high temperature furnaces and industrial heat exchangers for gas turbine engines [3-5]. Research is currently underway to develop cordierite as an alternative substrate to alumina for electronic applications [6-12].

Preparing dense cordierite glass-ceramics has long been a problem because of the narrow sintering range near cordierites incongruent melting point [12-14] and because of water molecules in the cavities of the cordierite structure which vaporize near the melting point leaving cracks and pores within the sintered body [6,12]. Low densities lead to inferior mechanical properties and consequently extensive research has been conducted to find ways of circumventing the problem. One answer was found with the use of sintering aids such as K_2O [6,15] or TiO_2 [16-20] which increased the density from less than 90% to 98% of theoretical. The drawback, however, was that these nucleating agents not only lowered the crystallization temperature and increased density but also increased the coefficient of thermal expansion

[1,2,5,21].

Other researchers focused on altering the synthesis techniques, specifically, utilizing a solution sol-gel (SSG) process [5,9-12,22-25] which was developed by Roy and co-workers in the early fifties [26-29] and has proven to be a breakthrough in ceramic processing. This technique allowed the preparation of fine reactive powders which can be crystallized and sintered at lower temperatures without the addition of impurities. Bernier and co-workers [10] obtained 96% densification of α-cordierite at a temperature of 1050°C although they failed to report the duration of sintering. Moyer and colleagues fired cordierite disks at 1400°C for 5 hours and found the density to be 97% of theoretical whereas the same result was achieved by Suzuki [12] after sintering for 2 hours at 1300°C. Each of these researchers utilized a variation of the solution sol-gel process.

More recently, 1982, Roy and Roy [30] developed a sol-gel process where the goal was to make compositionally diphasic gels which were heterogeneous on a nanometer scale rather than monophasic gels made from a homogeneous solution phase. This procedure involves combining discrete nanosized crystalline, semi-crystalline, or amorphous sols of different compositions and has been studied exclusively in binary systems such as Al_2O_3-MgO, Al_2O_3-SiO_2, $ZrSiO_4$ and $ThSiO_4$. An additional variation in the preparation of diphasic gels involves the addition of crystalline seeds which have the same composition and structure as the expected equilibrium phase. Gels of this type are structurally diphasic and the effect of seeding has been investigated for many binary systems including those described above.

As mentioned previously, the preparation of dense crystalline α-cordierite has long been a difficult and seemingly impossible task, however, through the use of nanocomposite gels this challenge may be met. The following study is an approach to lowering the crystallization temperature and enhancing densification of cordierite ceramics through the nanocomposite approach without the use of any sintering aids.

II. EXPERIMENTAL PROCEDURE

Three series of cordierite gels were prepared by the sol-gel route; a single

phase (monophasic) gel, a nominally triphasic gel prepared from two sols and one solution phase, and a truly triphasic gel made by combining three discrete sols. In addition, seeded preparations of the monophasic and triphasic gels were made for the crystallization study. The monophasic gel was prepared as follows: stoichiometric amounts of $Al(NO_3)_3 \cdot 9H_2O$ and $Mg(NO_3)_2 \cdot 6H_2O$ (Aldrich Chemicals) were separtely dissolved in ethyl alcohol. The solutions were then combined and to this mixture an appropriate amount of $Si(OC_2H_5)_4$, (TEOS), was added while stirring. The clear solution was allowed to gel in a 60°C water bath and then dried in a 100°C oven.

The second series of cordierite gel was prepared utilizing boehmite (Dispural, Remet Chemical Corp.) as the source of alumina which was dispersed in deionized water and peptized with 1N HNO_3 until an opalescent sol was obtained. A commercial silica sol (Ludox, E. I. du Pont de Nemours and Co.) was added while continuously stirring. A solution of $Mg(NO_3)_2 \cdot 6H_2O$ dissolved in deionized water was combined with the mixture of sols, again while stirring to maintain a uniform mix. The final milky sol was placed in a 100°C oven to dry.

The final preparation of cordierite gel was comprised of three distinct phases or sols, hence the name truly triphasic. As described for the other triphasic gel, stoichiometric proportions of the alumina sol and the silica sol were combined while stirring. The third component of this gel, however, was a magnesia sol rather than a magnesium solution. This sol was made by dispersing an appropriate amount of magnesia powder (UBE Industries) in deionized water and adding 1N HNO_3 until a colloidal suspension was obtained. The third component was then combined with the alumina-silica sol mixture, stirred for uniform mixing, and placed in a 100°C drying oven. After drying, each gel was calcined at 400°C to remove the volatiles such as nitrates and water.

The procedures described were used in the preparation of the three varieties of gels. Slight alterations were made to some of the cordierite gels to investigate other processing methods. Specifically, the effect of adding seed crystals to cordierite gels. For this study, two sets of the monophasic and triphasic gels were simultaneously prepared with one set of gels containing seeds. The seeds referred to here were crystalline α-cordierite seeds made from one of the dried monophasic gels which had been calcined at 400°C to remove the volatiles, ground to break up the aggregates and calcined at 1300°C to promote crystallization. The powder was then analyzed by x-ray

diffraction to ensure the material was single phase α-cordierite. The material was reground and passed through a -325 mesh sieve. Each of the seeded gels was prepared with 2% by weight of these crystalline seeds and following the procedure as previously described. For the monophasic gel, the crystalline particles were included with the aluminum nitrate solution and, for the nominally triphasic gel, the seeds were again incorporated in the beginning stages of preparation and combined with the alumina sol.

Once the synthesis of the powders was complete the next step was to investigate the phase evolution of the various powders and compare their crystallization behavior. The seeded and unseeded monophasic and triphasic powders were pressed into pellets at 175 MPa using a 6.4 mm diameter stainless steel die and Carver hydraulic press. The pellets were initially fired at 1000° and thereafter at 50°C increments until single phase α-cordierite resulted which was determined by powder x-ray diffraction utilizing Ni filtered CuKα radiation.

After analyzing the x-ray diffractograms, it was apparent that the addition of seeds had a favorable effect on the cordierite gels. A quantitative analysis was carried out to obtain more exact information about the amount of α-cordierite formed at each calcination temperature. The powder samples were mixed with the standard, Al_2O_3, in a weight ratio of 50:50 and examined again by x-ray diffraction. The area of the 100% intense peak of α-cordierite was compared to the area of the reference peak and the relative amount of crystalline α-cordierite was calculated.

In addition to studying the effects of seeding the gels, the goal of many experiments was to produce a more dense cordierite material. For this study, three varieties of cordierite gel powders were used; the monophasic gel, the triphasic gel, and the truly triphasic gel. Initially the powders were calcined at 600°C for 24 hours to remove any volatiles and then pressed into pellets at 175 MPa utilizing a 12.9 mm stainless steel die. The compacts were sintered in the ambient atmosphere of a programmable furnace and the final sintering temperature ranged from 1200° - 1400°C for a duration of 2 hours.

The densities of the sintered compacts were determined by a modified water immersion technique and encompass the volume of the solid material, the enclosed inner pores, and the open outer pores. The densities presented as the percent of theoretical were calculated from the JCPDS x-ray diffraction file of α-cordierite which lists the theoretical density as 2.512 g/ml. Following the

densification analysis, the pellets were analyzed by x-ray diffraction to ensure the compact was single phase α-cordierite. In addition, the fracture surface of the sintered pellets was examined to verify the density measurements, examine the pore and grain size, and check for homogeneity. The microstructures of the fracture surface were characterized with a scanning electron microscope (SEM).

III. RESULTS AND DISCUSSION

A. Phase Evolution

The monophasic and nominally triphasic gel powders in this study were calcined at 1000°C and thereafter at 50°C increments until single phase α-cordierite was formed. Figure 1 presents x-ray diffraction patterns of the calcined monophasic powder at 1000°, 1100°, 1200°, and 1250°C. The powder remained essentially amorphous at 1000°C, however, the onset of μ-cordierite crystallization can be observed by the peak at 25.9° 2θ. The XRD pattern of the 1100°C fired sample displayed crystallization peaks of both μ- and α-cordierite (10.4° 2θ). By 1200°C the monophasic gel powder had almost completely transformed into α-cordierite. The triphasic gel was simultaneously calcined with the monophasic gel powder and the x-ray diffraction patterns are displayed in Figure 2. The material fired at 1000°C showed two peaks at 36.9° and 44.8° 2θ which indicated the presence of spinel. However, no characteristic peaks of μ-cordierite were evident. Calcining the powder at 1100°C brought about the formation of cristobalite, identified by the peak occurring at 21.6° 2θ. By 1200°C the spinel and cristobalite phases had almost completely reacted to form α-cordierite except for a trace of spinel. Calcination of the triphasic powder at 1250°C resulted in single phase α-cordierite.

It is interesting to note the very different reaction paths of the two types of gels. The alkoxide derived gel progressed by the classical or well known path i.e., the formation of μ-cordierite followed by transformation to α-cordierite. The triphasic gel was prepared by combining colloidal suspensions and proceeded by the formation of spinel and cristobalite followed by reaction to α-cordierite.

B. Crystallization Study

The investigation aimed at determining if the addition of seed crystals would change the crystallization temperature was carried out on the monophasic and triphasic series of cordierite powder. Note that the seeded and unseeded varieties of gel powders were simultaneously fired in all cases to ensure identical firing temperatures and durations. The phases identified from the x-ray diffraction patterns are presented in Table 1. At temperatures where more than one phase were found to exist, they are listed in decreasing order of abundance. At 1075°C the monophasic gel was compised of α-cordierite, μ-cordierite, and spinel whereas the the seeded monophasic gel had formed α-cordierite with only a trace of spinel. By 1100°C the monophasic gel had not progressed, but the seeded counterpart had completely transformed to single phase α-cordierite. It was not until a calcination temperature of 1250°C that the monophasic gel powder transformed completely.

Examination of the triphasic series revealed a similar result. At 1100°C the triphasic powder was composed of cristobalite and spinel with no trace of α-cordierite whereas the seeded triphasic gel had already formed a large amount of α-cordierite in addition to cristobalite and spinel. By 1125°C some of the precursor phases had reacted to form α-cordierite in the unseeded gel while the reaction was complete in the seeded counterpart at this temperature. Again, it was not until 1250°C that the unseeded triphasic sample crystalized to single phase material.

This simple qualitative analysis was performed prior to quantifyiing the amount of crystalline α-cordierite and clearly illustrates the effect of including seed particles when preparing gels. Figure 3 is a plot of relative intensity versus calcination temperature for the monophasic series of gels. It is immediatly evident upon examination of the graph that the seeded gel formed a greater amount of α-cordierite at each of the calcination temperatures. In fact, at the initial firing temperature of 1000°C a substantial amount of α-cordierite already existed in the seeded monophasic gel whereas the unseeded sample had not even begun the transformation. By 1100°C the proportion of α-cordierite in the seeded gel had leveled off while the ratio in the unseeded counterpart was steadily increasing.

The quantitative analysis of the triphasic gels at various sintering temperatures is presented in Figure 4. As revealed for the monophasic gel, the

seeded triphasic gel powder displayed more crystalline α-cordierite at all temperatures than the unseeded variety. In addition, the onset of crystallization in the seeded sample occurred at 1050°C as evidenced by the measurable amount of α-cordierite at this temperature. The components of the unseeded triphasic gel did not react to form α-cordierite until 1125°C, but by this temperature the triphasic and seed powder had reached a plateau.

The results presented clearly support the well known nucleation and epitaxial growth mechanism [31-40]. Isostructural seed additions of the expected equilibrium phase provided nucleation sites upon which the amorphous material could grow. For the unseeded powders, energy is required to form these nuclei and therefore, by including seeds, the activation barrier for crystallization was lowered which led to the formation of the stable α-cordierite phase at lower temperatures. In addition, the utilization of seeds had a greater effect on the crystallization of α-cordierite in the monophasic gel as compared to the triphasic gel. This may be attributed to the excess free energy of the triphasic components.

C. Densification through Optimization of Heat Treatment

As mentioned previously, the ability to obtain dense cordierite ceramics is considered essential for many applications. Therefore, in addition to investigating the effect of seed additions into cordierite gels, an extensive study was undertaken to improve the final densities of sintered compacts. For this purpose, the three series of cordierite gels were utilized.

The difficulty of the study was determining the optimal heat treatments for the powders. For example, changing the prefiring temperature from 600°C to 400°C increased the densities of the sintered compacts which are presented in Table 2 for the monophasic and triphasic pellets. The explanation was found by considering the change in specific surface area with temperature. Suzuki et al. [5] reported that the surface area of alkoxide-derived gels gradually decreased at calcination temperatures below 800°C while Moyer et al. [23], utilizing colloidal sols, revealed that in the temperature range 400°-500°C the prepared cordierite gel exhibited a large surface area which strongly influenced the fired density ie., powders of high surface area yielded greenware of low density and sintered pieces of high density [23]. Note that the highest density, as measured for the triphasic powder prefired at 400°C and sintered at 1300°C, was 93.6% of

theoretical and although the change in processing technique demonstrates a slight improvement, the density remained substantialy less than the values reported in the literature.

Another step of the heat treatment which required additional investigation was in the temperature range 760°-830°C. Many researchers conducted thermal dilatometric measurements and reported that cordierite exhibits abrupt densification in this temperature inteval [4,10,11]. Scanning electron micrographs of samples quenched from this firing range illustrated coalescing of the particles and smoothing of the rough surfaces resulting from a viscous flow mechanism [7,9,11]. Barry and co-workers [17] slowly heated specimens from 780°-830°C and measured the strength of the fired material. They reported that a slow heating rate from 780°C allowed efficient nucleation and initial crystallization to take place which resulted in a stronger fired compact.

As a result of this finding, alterations were made to the original firing schedule to incorporate a period of slow heating prior to crystallization. The temperature range and heating rate were varied until optimum densification was achieved. The firing program utilized to sinter the cordierite pellets is presented in Figure 5 although the final sintering temperature varied from 1200°-1400°C. Table 3 presents the calculated densities as well as the percent of theoretical. At 1300°C the monophasic and nominally triphasic pellets exhibited densities of 80 and 96% respectively, and although the triphasic compact attained a reasonable density without the use of a sintering aid, the result is overshadowed by the density attained by the truly triphasic powder, 100% of theoretical. These results are presented graphically in Figure 6 where the changes in densification are more apparent. The plot displays densities which are greater than theoretical for the truly triphasic gel at temperatures below 1300°C. This discrepancy can be explained by powder x-ray diffraction results which revealed that the sintered pellets are composed, not only of α-cordierite but of the phases which are known to preceed α-cordierite formation. The densities of proportional amounts of spinel and cristobalite are greater than that of pure cordierite which led to the higher densities. Powder x-ray diffraction assured that the 1300°C compacts were comprised of single phase α-cordierite. Further examination of the plot reveals a reduction in density near 1400°C. A similar result was documented by Suzuki et al. [12] who attributed the decrease in density to water molecules which were positioned within the cavaties of the cordierite structure. As the cordierite pellets are sintered above

1400°C, the vapor pressure of the water increases expanding the cavities leaving cracks and pores within the compact. In addition, high temperature mass spectroscopy showed N_2 gas evolving from the sintered pellets at temperatures greater than 1200°C [6,9].

In conjuction with density measurements, examination of the microstructure of fractured surfaces reveals information about densification behavior and porosity. Micrographs of fracture surfaces are displayed in Figure 7 for each series of powder sintered at 1300°C for 2 hours. The monophasic microstructure (Figure 7a) showed densification by viscous flow mechanism as evidenced by the coalescing of particles and the rounded edges. The micrograph displays the surface of a poorly sintered material with an appreciable amount of macroporosity, which is in agreement with the measured density (80% of theoretical density). The fracture surface of the triphasic pellet in Figure 7b revealed the formation of a much denser material (96% of theoretical density). There is good cohesion between particles with some intergranular pores. However, the triphasic material exhibits a substantial improvement in sintering behavior over the monophasic sample. The micrograph of most interest was that of the 100% dense truly triphasic compact which was expected to reveal complete densification. Examination of Figure 7c does in fact coincide with the measured density in that there was a notable lack of porosity and good cohesion. It can be concluded that the truly triphasic material clearly exhibits excellent sintering and densification.

The enhanced sinterability of cordierite bodies through the use of ultrafine homogeneous powders rather than single phase solution sol-gels is due to excess free energy. Triphasic gels store more excess free energy because of the added heat of reaction of the separate precursor phases as well as the contribution from increased surface energy on the individual powders [34,39-41]. By applying this theory to the cordierite system, the differing densities attained for each series of gel powders can be reasonably explained.

CONCLUSIONS

The applications of cordierite as a ceramic material are limited by poor mechanical properties which directly result from the inability to sinter cordierite. The inclusion of α-cordierite seed particles when preparing the gels was not

effective in increasing the final density of the material but was extremely successful in lowering the crystallization temperature of α-cordierite. Lower processing temperatures may extend the uses of cordierite particularly in the electronics industry where multilayered substrates are cofired with low melting metallic conductors. Adding seeds lowered the processing temperature at which the transformation to single phase α-cordierite was complete by as much as 150°C.

Enhancing densification was an important and beneficial goal which would improve the mechanical properties of cordierite ceramics. The utilization of ultafine homogeneous powders when preparing the gels not only eliminated comminuting of the powders and maintained their high purity but also allowed complete densification without the use of sintering aids due to their high reactivity.

ACKNOWLEDGMENTS

Financial support for this research was provided by the Air Force Office of Scientific Research under Contract No. F49620-88-C-0134.

REFERENCES

[1]I. M. Lachman, R. D. Bagley and R. M. Lewis, Ceram. Bull. **60** (2), 202 (1981).

[2]H. Ikawa, T. Otagiri, O. Imai, M. Suzuki, K. Urabe, and S. Udagawa, J. Am. Ceram. Soc. **69** (6), 492 (1986).

[3]Y. Hirose, H. Doi and O. Kamigaito, J. Mater. Sci. Lett. **3**, 153 (1984).

[4]R. J. Higgins, H. K. Bowen, and E. A. Giess, in *Advances in Ceramics*, edited by G. L. Messing, K. S. Mazdiyasni, J. W. McCauley and R. A. Haber (American Ceramic Society, Westerville, OH, 1987), Vol. 21, p. 691.

[5]H. Suzuki, K. Ota and H. Saito, Yogyo-Kyokai-Shi, **95** (2), 25 (1987).

[6]B. H. Mussler and M. W. Shafer, Ceram. Bull. **63** (5), 705 (1984).

[7]K. Watanabe and E. Giess, J. Am. Ceram. Soc. **68** (4), C-102 (1985).

[8]K. Watanabe, E. A. Giess and M. W. Shafer, J. Mater. Sci. **20** (2), 508 (1985).

[9]C. Gensse and U. Chowdhry, in *Better Ceramics Through Chemistry II*, edited by C. J. Brinker, D. E. Clark, and D. R. Ulrich (Materials Research Society, Pittsburgh, 1986), Mater. Res. Soc. Symp. Proc., Vol.73, p. 693.

[10]J. C. Bernier, J. L. Rehspringer, S. Vilminot and P. Poix, in *Better Ceramics Through Chemistry II*, edited by C. J. Brinker, D. E. Clark, and D. R. Ulrich (Materials Research Society, Pittsburgh, 1986), Mater. Res. Soc. Symp. Proc., Vol.73, p. 693.

[11]H. Vesteghem, A. R. Di Giampaolo and A. Dauger, J. Mater. Sci. Lett. **6**, 1187 (1987).

[12]H. Suzuki, K. Ota and H. Saito, Yogyo-Kyokai-Shi **95** (2), 32 (1987).

[13]R. S. Lamar and M. F. Warner, J. Am. Ceram. Soc. **37** (12), 602 (1954).

[14]R. Morrell, *Proc. Brit. Ceram. Soc.* **28**, 53 (1979).

[15]D. M. Miller, Corning Glass Works, Corning, NY, United States Patent 3,926,648 (1975).

[16]A. G. Gregory and T. J. Veasey, J. Mater. Sci. **6** (10), 1312 (1971).

[17]T. I. Barry, L. A. Lay and R. Morrell, Sci. Ceram. **8**, 331 (1976).

[18]J. S. Thorp and W. Hutton, J. Phys. Chem. Solids **42**, 843 (1981).

[19]J. S. Thorp and W. Hutton, J. Phys. Chem. Solids **44**, 1039 (1983).

[20]W. Hutton and J. S. Thorp, J. Mater Sci. **20** (2), 542 (1985).

[21]G. H. Beall, in *Advances in Ceramics*, edited by D. C. Boyd and J. F. MacDowell (American Ceramic Society, Columbus, OH, 1986), Vol. 18, p. 157.

[22]B. J. J. Zelinski, B. D. Fabes and D. R. Uhlmann, J. Non-Cryst. Solids **82**, 307 (1986).

[23]J. R. Moyer, A. R. Prunier, Jr., N. N. Hughes and R. C. Winterton, in *Better Ceramics Through Chemistry II* , edited by C. J. Brinker, D. E. Clark, and D. R. Ulrich (Materials Research Society, Pittsburgh, 1986), Mater. Res. Soc. Symp. Proc., Vol. 73, p. 117.

[24]R. M. Smart and F. P. Glasser, J. Mat. Sci., **11**, 1459 (1976).

[25]L. A. Paulick, Y. Yu and T. Mah, in *Advances in Ceramics*, edited by G. L. Messing, K. S. Mazdiyasni, J. W. McCauley and R. A. Haber (American Ceramic Society, Westerville, OH, 1987), Vol. 21, p.121.

[26]R. Roy and E. F. Osborn, Am. Mineral. **39** (11/12), 853 (1954).

[27]V. G. Hill, R. Roy, and E. F. Osborn, J. Am. Ceram. Soc. **35** (6), 135 (1952).

[28]D. M. Roy and R. Roy, Am. Mineral. **39** (11/12), 957 (1954).

[29]R. Roy, J. Am. Ceram. Soc. **39** (4), 145 (1956).

[30]R. A. Roy and R. Roy, Abstracts, Annual Meeting of Materials Research Society, (Boston, MA, 1982) p. 377.

[31]M. Kumagi and G. L. Messing, J. Am. Ceram. Soc. **67** (11), C-230 (1984).

[32]M. Kumagi and G. L. Messing, J. Am. Ceram. Soc. **68** (9), 500 (1985).

[33]Y. Suwa, R. Roy and S. Komarneni, J. Am. Ceram. Soc. **68** (9), C-238 (1985).

[34]R. Roy, Y. Suwa and S. Komarneni, in *Science of Ceramic Chemical Processing*, edited by L. L. Hench and D. R. Ulrich (John Wiley & Sons, New York, NY, 1986), p. 247.

[35]G. L. Messing, M. Kumagai, R. A. Shelleman and J. L. McArdle, in *Science of Ceramic Chemical Processing*, edited by L. L. Hench and D. R. Ulrich (John Wiley & Sons, New York, NY, 1986), p. 259.

[36]Y. Suwa, S. Komarneni and R. Roy, J. Mater. Sci. Lett. **3**, 21 (1986).

[37]Y. Suwa, R. Roy and S. Komarneni, Mater. Sci. Eng. **83**, 151 (1986).

[38]S. Komarneni, Y. Suwa and R. Roy, J. Mater. Sci. Lett. **6**, 525 (1987).

[39]G. Vilmin, S. Komarneni and R. Roy, J. Mater. Res. **2** (4), 489 (1987).

[40]R. Roy, S. Komarneni and W. Yarbrough, in *Ultrastructure Processing of Advanced Ceramics*, edited by J. D. Mackenzie and D. R. Ulrich (John Wiley & Sons, New York, NY, 1988), p. 571

[41]S. Komarneni, Y. Suwa and R. Roy, J. Am. Ceram. Soc. **69** [7] C155 (1986).

FIG 1. Phase evolution of α-cordierite from a monophasic gel.

FIG 2. Phase evolution of α-cordierite from a triphasic gel.

FIG 3. Relative amount of crystalline α-cordierite versus calcination. temperature for monophasic series of powders.

FIG 4. Relative amount of crystalline α-cordierite versus calcination temperature for triphasic series of powders.

FIG 5. Schematic of the optimal firing schedule.

FIG 6. Graphical representation of densities obtained after sintering for 2 hours.

FIG7. Scanning electron micrographs of fracture surfaces from pellets sintered at 1300°C for 2 hours. (a) monophasic, (b) triphasic and (c) truly triphasic.

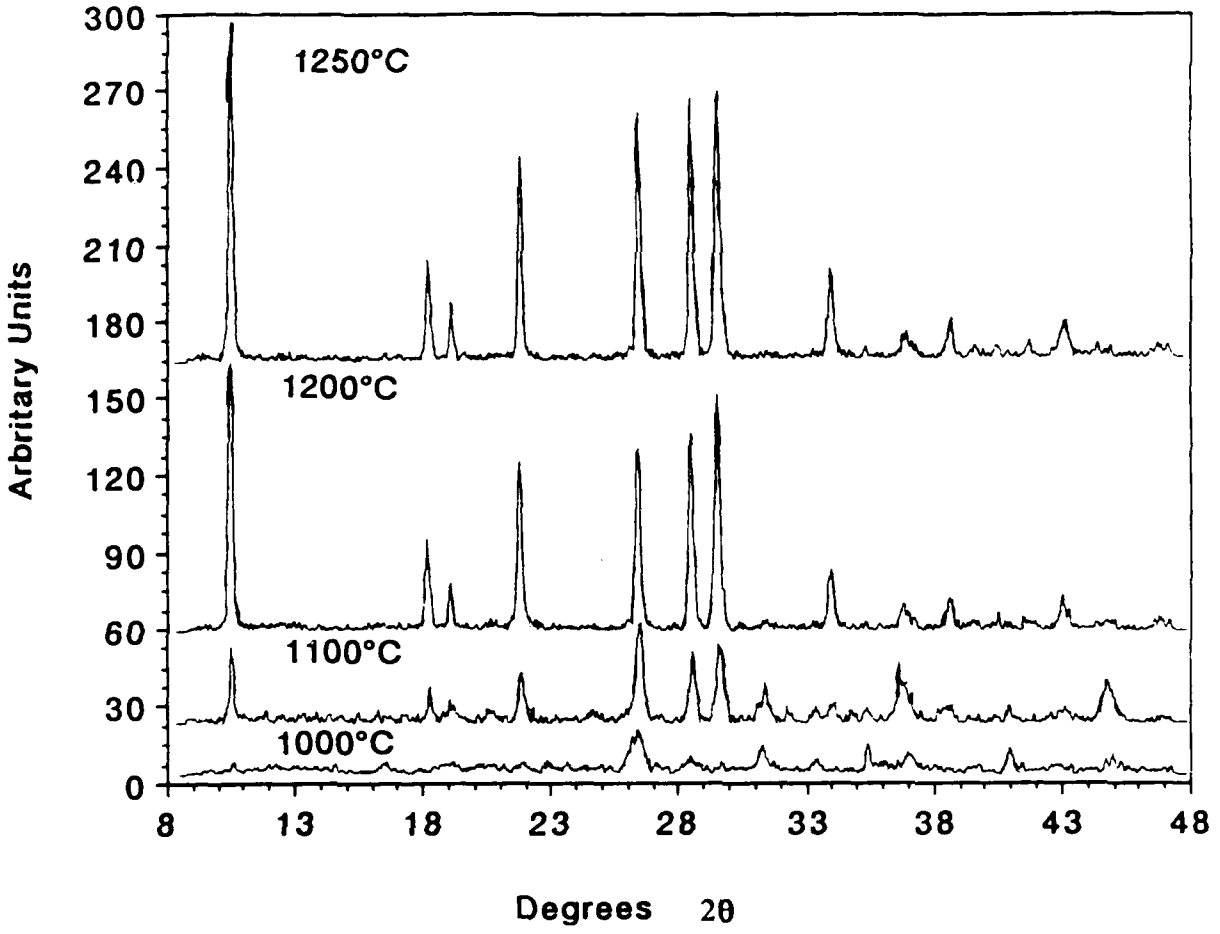
300
270
240
210
180
150
120
90
60
30
0
Arbritary Units
1250°C
1200°C
1100°C
1000°C
8
13
18
23
28
33
38
43
48
Degrees 2θ

Figure 1.

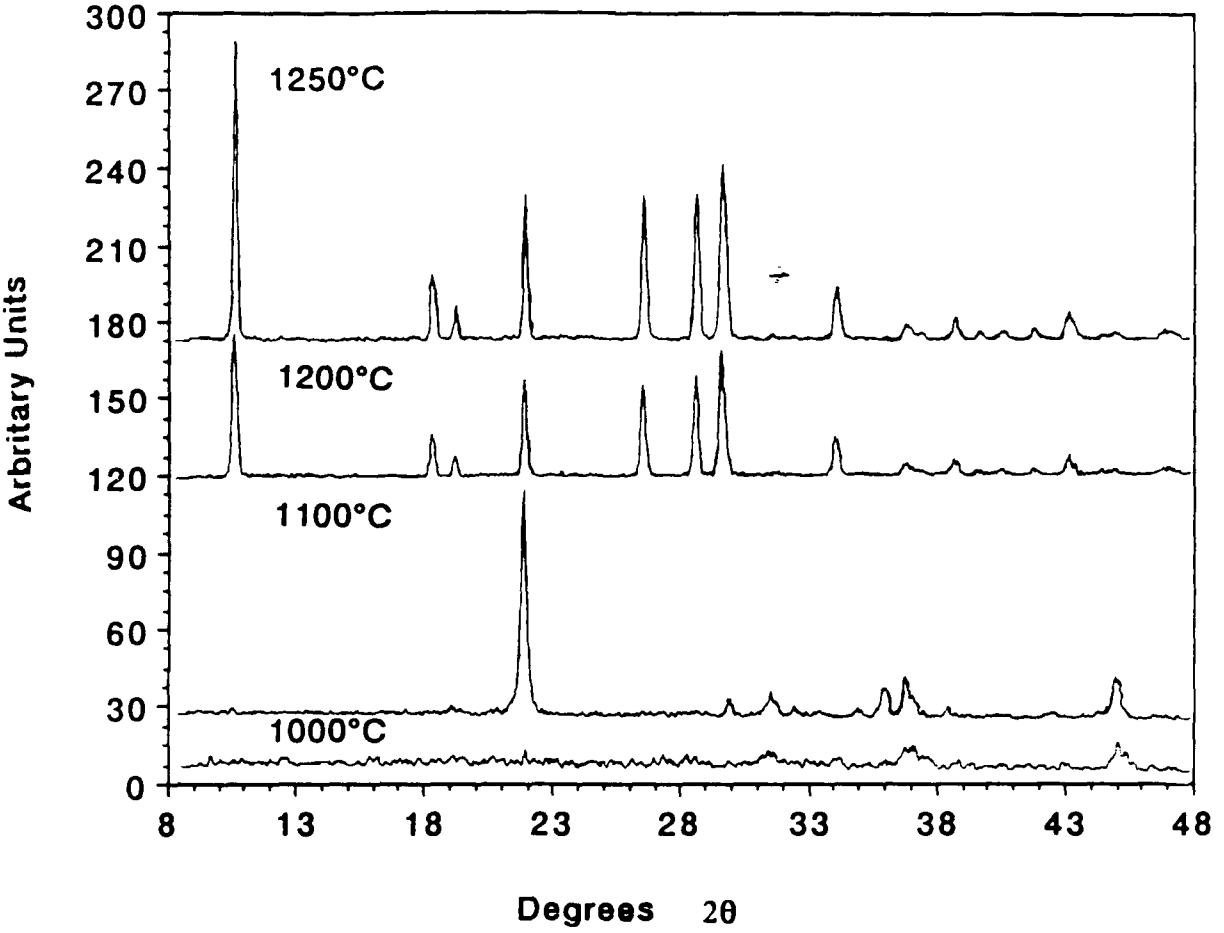
300
270
240
210
180
150
120
90
60
30
0
Arbitary Units
1250°C
1200°C
1100°C
1000°C
8
13
18
23
28
33
38
43
48
Degrees 2θ

Figure 2.

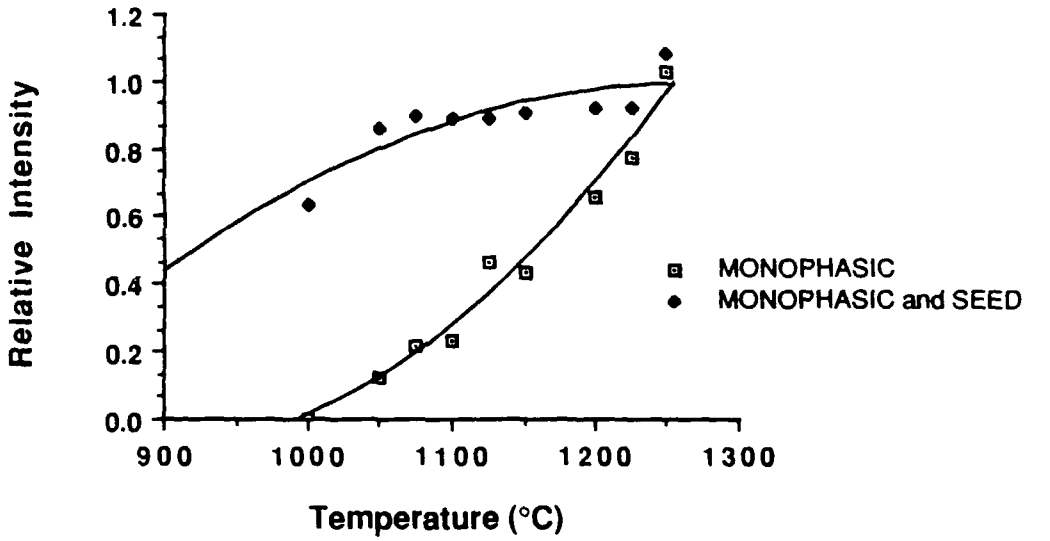
Relative Intensity
1.2
1.0
0.8
0.6
0.4
0.2
0.0
900
1000
1100
1200
1300
Temperature (°C)
MONOPHASIC
MONOPHASIC and SEED

Figure 3.

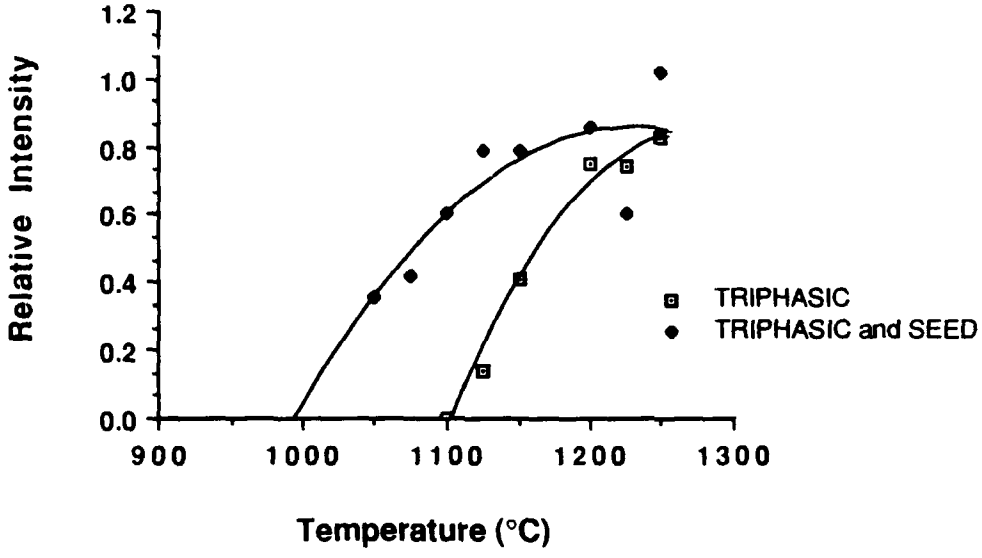
Relative Intensity
1.2
1.0
0.8
0.6
0.4
0.2
0.0
900
1000
1100
1200
1300
Temperature (°C)
TRIPHASIC
TRIPHASIC and SEED

Figure 4.

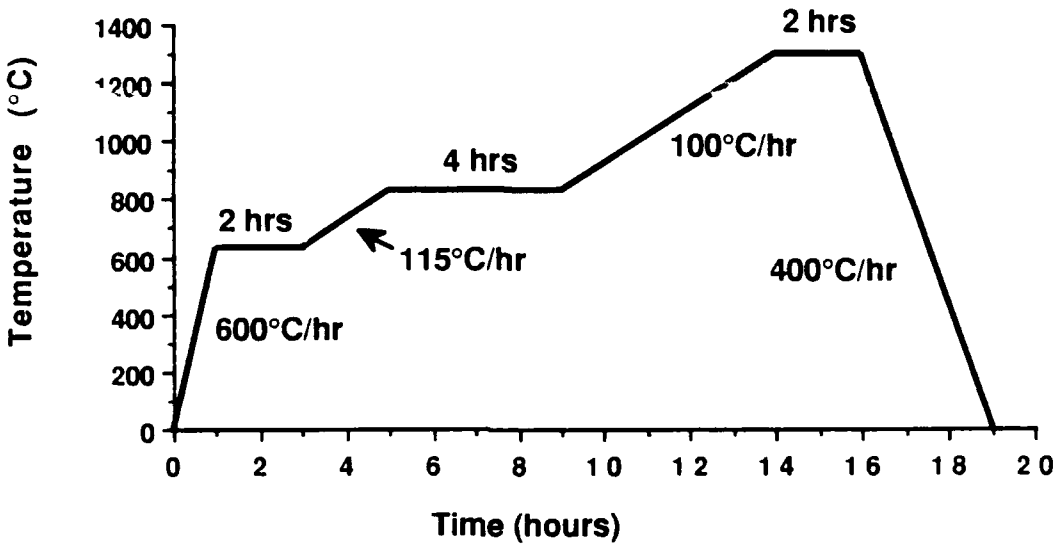
Temperature (°C)
1400
1200
1000
800
600
400
200
0
0
2
4
6
8
10
12
14
16
18
20
Time (hours)
2 hrs
600°C/hr
4 hrs
115°C/hr
100°C/hr
2 hrs
400°C/hr

Figure 5.

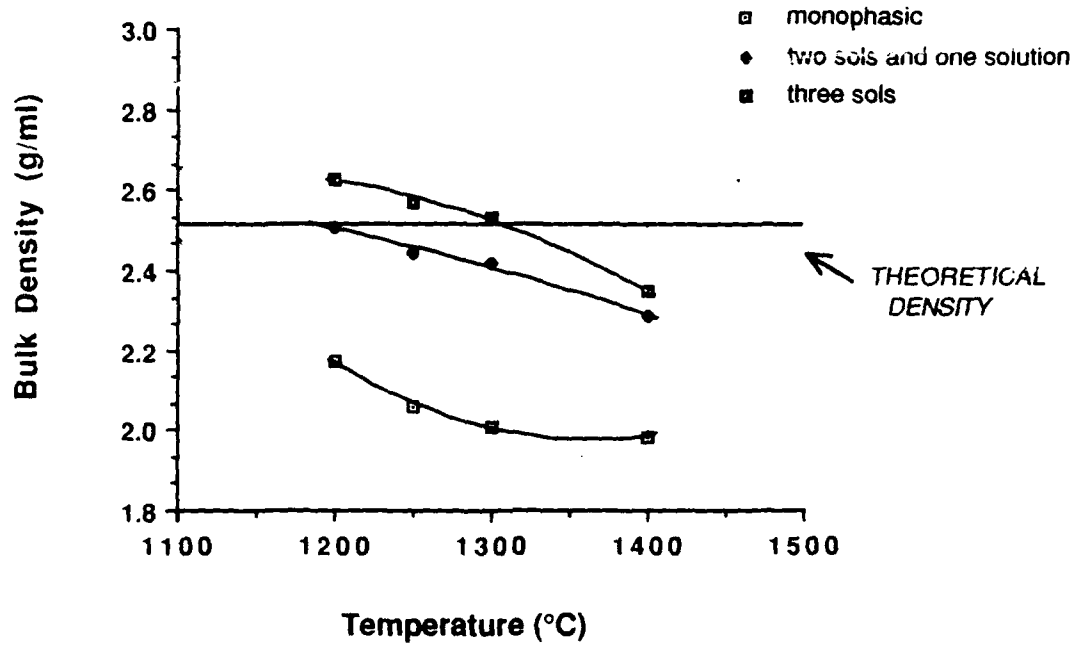
monophasic
two sols and one solution
three sols
THEORETICAL DENSITY
Bulk Density (g/ml)
3.0
2.8
2.6
2.4
2.2
2.0
1.8
1100
1200
1300
1400
1500
Temperature (°C)

Figure 6.

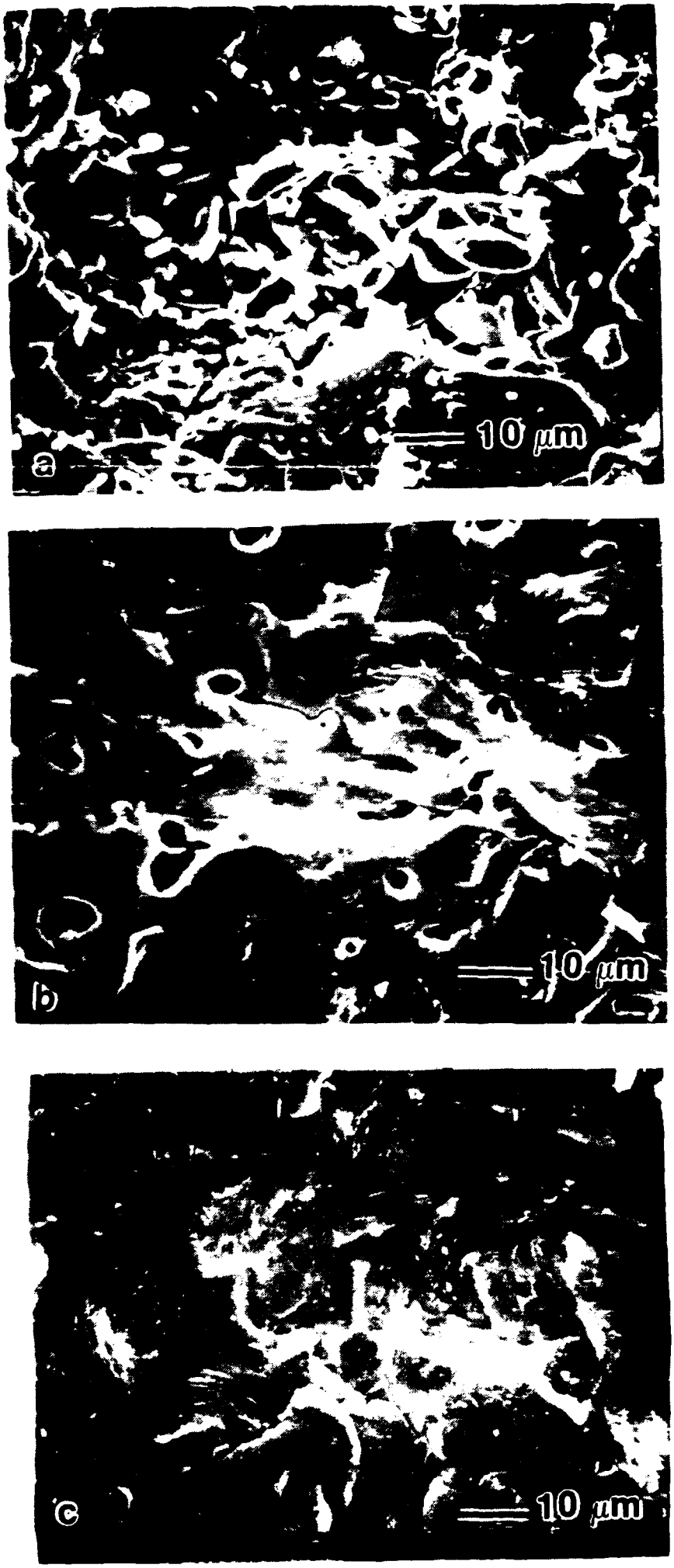

Figure 7.

TABLE I. Phases identified by powder x-ray diffraction at various sintering temperatures.

Temp. (°C)	Monophasic	Monophasic and Seed	Triphasic	Triphasic and Seed
1000°	amorphous μ-cordierite	α-cordierite μ–cordierite	amorphous	amorphous
1100°	μ-cordierite α-cordierite	α-cordierite μ–cordierite	cristobalite spinel	cristobalite spinel
1150°	α-cordierite μ–cordierite	α-cordierite trace spinel	cristobalite spinel	α-cordierite cristobalite spinel
1200°	α-cordierite μ–cordierite trace spinel	α-cordierite	α-cordierite cristobalite spinel	α-cordierite cristobalite spinel
1300°	α-cordierite	α-cordierite	α-cordierite	α-cordierite

TABLE II. Comparison of densities obtained from varying the prefire temperature.

Temperature	Monophasic	Triphasic
Prefired at 600°C	2.30 g/ml	2.33 g/ml
	91.6%	92.8%
Prefired at 400°C	2.33 g/ml	2.35 g/ml
	92.8%	93.6%

TABLE III. Densities obtained after sintering for 2 hours.

Temp. (°C)	Monophasic (solution sol-gel)	Triphasic (two sols and one solution)	Truly Triphasic (three sols)
1200°	2.17 g/ml	2.51 g/ml	2.63 g/ml
	86.5%	100.0%	104.7%
1250°	2.06 g/ml	2.44 g/ml	2.57 g/ml
	82.0%	97.2%	102.3%
1300°	2.01 g/ml	2.42 g/ml	2.52 g/ml
	80.0%	96.3%	100.2%
1400°	1.98 g/ml	2.29 g/ml	2.35 g/ml
	79%	91.0%	93.5%

MANUSCRIPT #3

Preparation and Densification of Forsterite (Mg_2SiO_4) by Nanocomposite Sol-Gel Processing

PREPARATION AND DENSIFICATION OF FORSTERITE (Mg_2SiO_4) BY NANOCOMPOSITE SOL-GEL PROCESSING

ANN KAZAKOS, SRIDHAR KOMARNENI, AND RUSTUM ROY

Materials Research Laboratory, The Pennsylvania State University, University Park, PA 16802.

ABSTRACT

A diphasic nanocomposite sol-gel processing has become an excellent way of producing stoichiometric homogeneous powders with many advantages over the solid state reaction method as well as the solution sol-gel method. This procedure is described for forsterite, Mg_2SiO_4, and the resulting densities of 97% for the diphasic and 91% for the monophasic gel powder are reported. In addition, a small amount of enstatite, $MgSiO_3$, was detected which is consistent with the findings of earlier researchers.

INTRODUCTION

The concept of preparing gels from ultrafine or nanoscale precursors was described by Roy and Roy in 1982 [1] and continues to be an optimal method for producing highly dense ceramics. The di- or multiphasic nanocomposite procedure involves making sols from ultrapure powders and then combining the sols in stoichiometric proportions depending on the desired phase. The familiar solution sol-gel process (SSG) is also an excellent way of producing pure

homogeneous ceramic powders due to the atomic scale mixing "inherent" in these gels. It has been demonstrated that this intimate interaction can lower the crystallization temperature by hundreds of degrees when compared to the traditional solid state reaction method. However, the SSG method in some cases necessitates tedious refluxing and careful hydrolysis of the precursor alkoxides in order to achieve proper mixing, whereas the nanosized powders are simply mixed with water, peptized to form a sol, and combined.

David Johnson [2] carefully reviewed sol-gel processing and categorized the different SSG methods in use today. He described the all alkoxide or solution sol-gel route as well as the colloidal sol or nanocomposite route. The review stated that one characteristic of multiphasic gels is the small shrinkage upon drying which leads to the formation of large crack-free bodies. This is a distinct advantage as it enables colloidal gels to be molded, gelled, and dried into a variety of shapes opening the door for any number of industrial applications.

The multiphasic nanocomposite route has been used to form ceramic powders or bodies for the unary system Al_2O_3 [3,4] and binary systems such as: Al_2O_3-MgO [5,6], Al_2O_3-SiO_2 [7], ThO_2-SiO_2 [8] and ZrO_2-SiO_2 [9] systems. More recently the advantage of utilizing colloidal sols has been reported for the quaternary MgO-Al_2O_3-SiO_2 system [10,11]. However Higgens et al. [10], combined a spinel (magnesium aluminate) sol and a silica sol whereas Kazakos et al. [11] prepared three distinct colloidal sols.

This paper describes yet another system where nanoscale powders were used as the precursors for gel formation. We report on the preparation of forsterite, Mg_2SiO_4, via the monophasic or single phase (nitrate alkoxide) and colloidal sol techniques and compare the final bulk densities obtained for each method.

EXPERIMENTAL

The single phase Mg_2SiO_4 gel was prepared by dissolving $Mg(NO_3)_2{\cdot}6H_2O$ in absolute ethanol after which an appropriate amount of tetraethoxysilane was added while stirring. The clear solution was placed in a 60°C water bath to promote gelation. The clear gel was dried at 100°C and then ground by hand with a mortar and pestle. A schematic is presented in Figure 1a and 1b for the preparation of monophasic and diphasic gels, respectively.

The diphasic gel was made by combining colloidal sols of each of the constituents. Ultrafine high purity magnesia powder, obtained from UBE Industries, Ltd. Japan, was added to water and stirred until the mixture resembled an opalescent colloidal suspension. A stoichiometric proportion of a commercial silica sol (Ludox, E. I. DuPont de Nemours and Co., Inc., Wilmington, DE) was added while stirring. The mixture was then placed in a 100°C drying oven after which the powder was ground by hand to break up the large pieces.

Each powder was then calcined at 400°C for several hours to remove the volatiles and later reground. The powders were pressed into 13 mm diameter pellets at 175 MPa for use in the sintering studies. To maintain consistency, 0.5 mg of powder was weighed for each pellet. A programmable furnace was utilized to achieve stepwise heating in air with variations in the final firing temperature.

After sintering, the density of each forsterite piece was found by the Archimedes method with water as the displacement liquid. Prior to the density

measurement, each pellet was thinly coated with household paraffin to prevent water from entering the pores. In this way, the density of the ceramic body could be determined as it would be manufactured i.e., including any holes or pores that might form. An additional analysis that is vital to this study includes characterization by powder x-ray diffraction. For this purpose, a Scintag/USA Model #PAD-V diffractometer with CuKα radiation was utilized. It is important to identify the crystalline phases formed at each sintering temperature.

RESULTS AND DISCUSSION

The density of the sintered pellets as measured for the monophasic and diphasic routes are plotted in Figure 2 for various temperatures and each heated for a 1 hour duration. The theoretical density used as a reference was obtained from the JCPDS file card of Mg_2SiO_4 and given as 3.22 g/ml. The densities, presented as percent of theoretical, are given in Table 1. Densification appears to be complete near 1200°C where the measured densities for values are 97.5% for the diphasic gel powder and 91.0% for the single phase gel powder. However, further analysis and phase identification of the crystalline material is necessary and is reported below. Note that the densities remain constant over several hundred degrees before decreasing slightly around 1500°C. The results clearly demonstrate the enhanced densification obtained when forsterite is prepared utilizing diphasic gels as compared to monophasic or single phase gels. The enhanced densification of diphasic gels may be attributed to the heat of reaction contributed by the discrete phases at the sintering temperature as has been suggested before by us [7,11].

Powder x-ray diffractometry was performed on each of the samples to determine which phases were present. Figure 3 presents x-ray diffraction patterns of the monophasic and diphasic gel powders fired at 1100°C. The analysis showed that a substantial amount of forsterite was formed at 1100°C in the monophasic sample while the diphasic powder crystallized completely at the same temperature. As the firing temperature was increased to 1200°C the single phase powder had completely crystallized, however, the powder prepared from colloidal sols displayed a very small amount of enstatite, $MgSiO_3$ as depicted in Figure 4. Further heat treatment did not have any apparent effect on the enstatite phase until a firing temperature near 1600°C was reached, which is above the melting point of enstatite. In a separate experiment, it was found that the crystallization of enstatite could not be detected until a firing temperature of 1200°C was reached.

Careful examination of the diffraction pattern failed to reveal any peaks corresponding to MgO. Therefore, in order to obtain a phase pure material, the diphasic gel was remade with up to 5% by weight excess MgO powder assuming that the preparation was not stoichiometric. This experiment proved inconclusive as the enstatite phase persisted throughout the sintering cycle.

A paper by Brindley and Hayomi [12] discussed the formation of forsterite (Mg_2SiO_4) by solid state reaction between MgO and SiO_2. They utilized x-ray diffraction, electron probe, and cathodo-luminescence observations to determine that, although forsterite is the main product formed in each of the experiments, a layer of enstatite was found between forsterite and the SiO_2 phase. The authors concluded that MgO diffuses into the open silica structure and initially forms the enstatite phase. The MgO continues to diffuse through the thin enstatite layer and results in the final product, forsterite.

The same reaction sequence is believed to occur in the diphasic gel prepared for this study. The powders used by Brindley were roughly micron size whereas the colloidal sols described in this paper were made from nanometer size particles. However, the concept of a solid state reaction between discrete MgO and SiO_2 is maintained. Further work revealed that soaking times of up to 30 hours at 1200°C were sufficient to eliminate the enstatite phase. Note that the monophasic powder did not exhibit the same tendencies since the solution sol-gel proceeds by atomic scale mixing rather than discrete particle interactions.

CONCLUSIONS

Virtually phase pure dense forsterite bodies were easily prepared by mixing colloidal sols and sintering to a temperature of 1200°C and higher. However, a small amount of enstatite was detected in this temperature range when heated for short duration which is In agreement with work by other researchers. Since the theoretical density of enstatite (3.19 g/ml) approaches that of forsterite, and because there was only a few percent of this second phase, no correction was made. The resulting densities were greater than 97% of theoretical for the diphasic powder and 91% for the monophasic preparation, the enhanced densification of the former is attributed, at least in part, to the heat of reaction contributed by the discrete phases.

ACKNOWLEDGEMENT

This research was supported by the U.S. Air Force Office of Scientific Research under contract No. F49620-88-C-0134.

REFERENCES

[1]R. A. Roy and R. Roy, Abstracts, New Metal Ceramic Hybrid Xerogels, Annual Meeting of Materials Research Society, (Boston, MA, 1982) p. 377.
[2]D. W. Johnson, Jr., Ceram. Bull., **64** (12), 1597 (1985).
[3]Y. Suwa, S. Komarneni and R. Roy, J. Mater. Sci. Lett. **5**, 21 (1986).
[4]Y. Suwa, R. Roy and S. Komarneni, Mater. Sci. Eng. **83**, 151 (1986).
[5]D. Hoffman, R. Roy and S. Komarneni, Mater. Lett., **2**, 245 (1984).
[6]S. Komarneni, Y. Suwa and R. Roy, J. Mater. Sci. Lett. **6**, 525 (1987).
[7]S. Komarneni, Y. Suwa and R. Roy, J. Am. Ceram. Soc. **69** [7] C155 (1986).
[8]G. Vilmin, S. Komarneni and R. Roy, J. Mater. Res. **2** (4), 489 (1987).
[9]G. Vilmin, S. Komarneni and R. Roy, to be published
[10]R. J. Higgins, H. K. Bowen, and E. A. Giess, in *Advances in Ceramics*, edited by G. L. Messing, K. S. Mazdiyasni, J. W. McCauley and R. A. Haber (American Ceramic Society, Westerville, OH, 1987), Vol. 21, p. 691.
[11]A. Kazakos-Kijowski, S. Komarneni and R. Roy, in *Better Ceramics Through Chemistry III*, edited by C. J. Brinker, D. E. Clark, and D. R. Ulrich (Elsevier Science Publishing Co., New York, NY, 1987), p.245.
[12]G. W. Brindley and R. Hayami, Phil. Mag. **12** (117), 505 (1965).

TABLE I. Comparison of densities obtained from varying the final sintering temperature.

Temperature	Monophasic	Diphasic
1100°C	81.2%	88.0%
1200°C	91.1%	97.5%
1300°C	90.2%	97.3%
1400°C	91.1%	97.4%
1500°C	89.4%	95.8%

Figure 1. Flow charts for the preparation of (a) monophasic gel and (b) diphasic sol

Figure 2. Plot of density versus sintering temperature for the monophasic and diphasic powders with a soak time of 1 hour

Figure 3. Powder x-ray diffraction patterns of (a) monophasic and (b) diphasic pellets after sintering at 1100°C for 1 hour

Figure 4. Powder x-ray diffraction pattern after sintering the diphasic preparation for 1 hour at 1200°C.

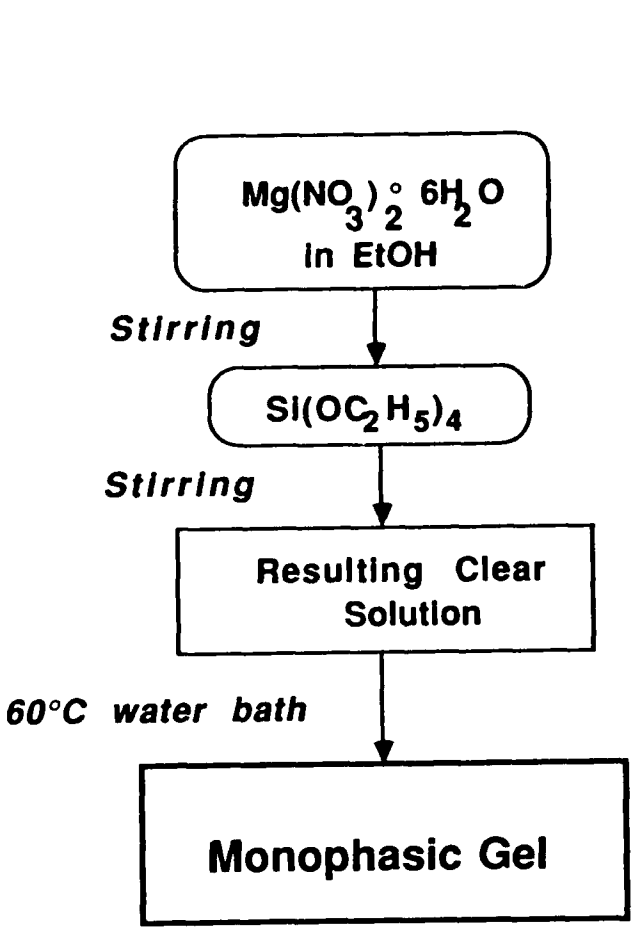
$Mg(NO_3)_2 \cdot 6H_2O$
in EtOH
Stirring
$Si(OC_2H_5)_4$
Stirring
Resulting Clear Solution
60°C water bath
Monophasic Gel

(a)

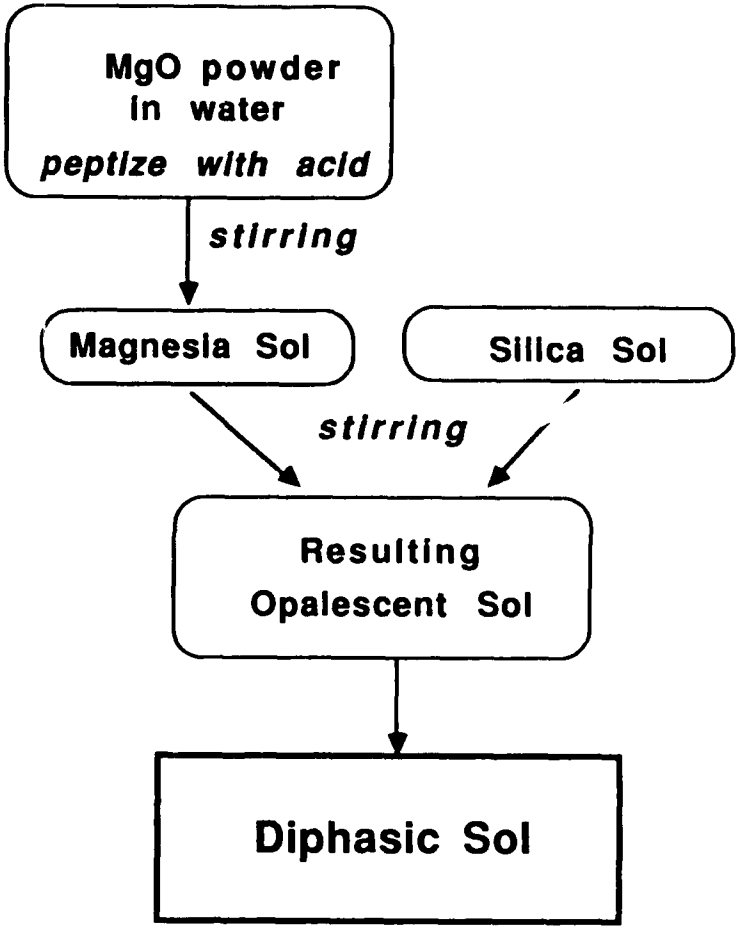
MgO powder
in water
peptize with acid
stirring
Magnesia Sol
Silica Sol
stirring
Resulting Opalescent Sol
Diphasic Sol

(b)

Figure 1.

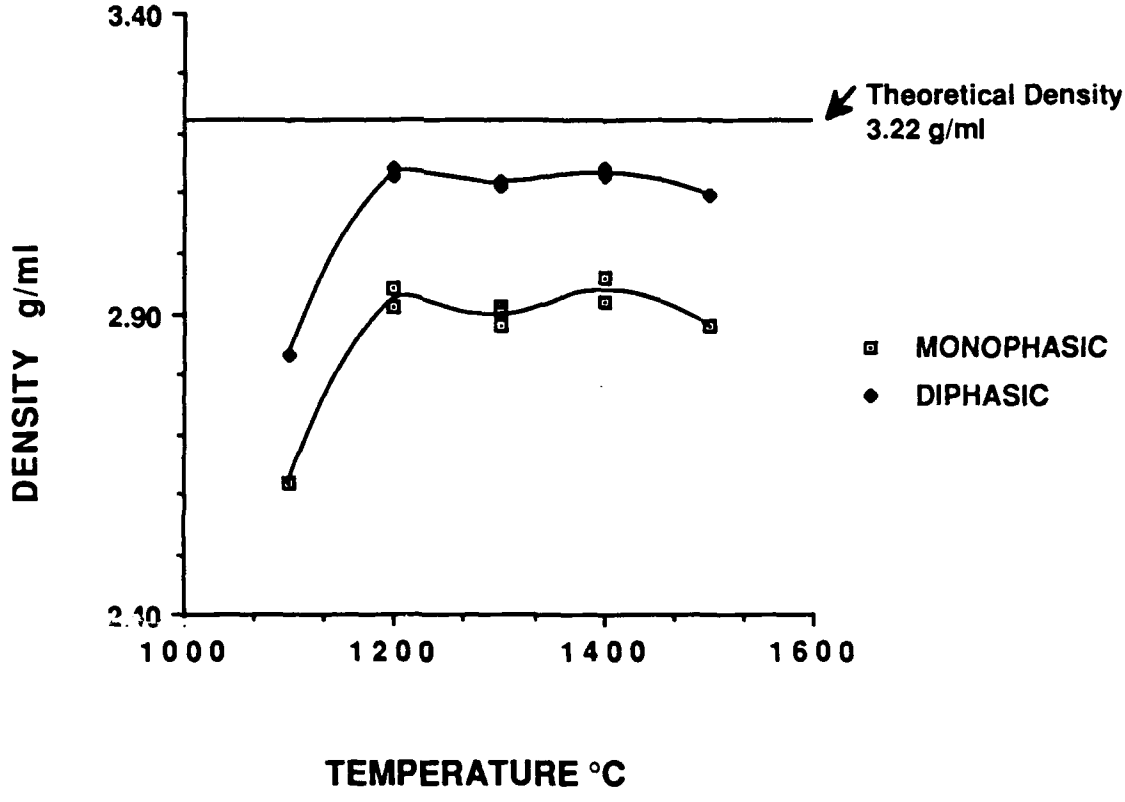
3.40
2.90
2.40
DENSITY g/ml
1000
1200
1400
1600
TEMPERATURE °C
Theoretical Density
3.22 g/ml
MONOPHASIC
DIPHASIC

Figure 2.

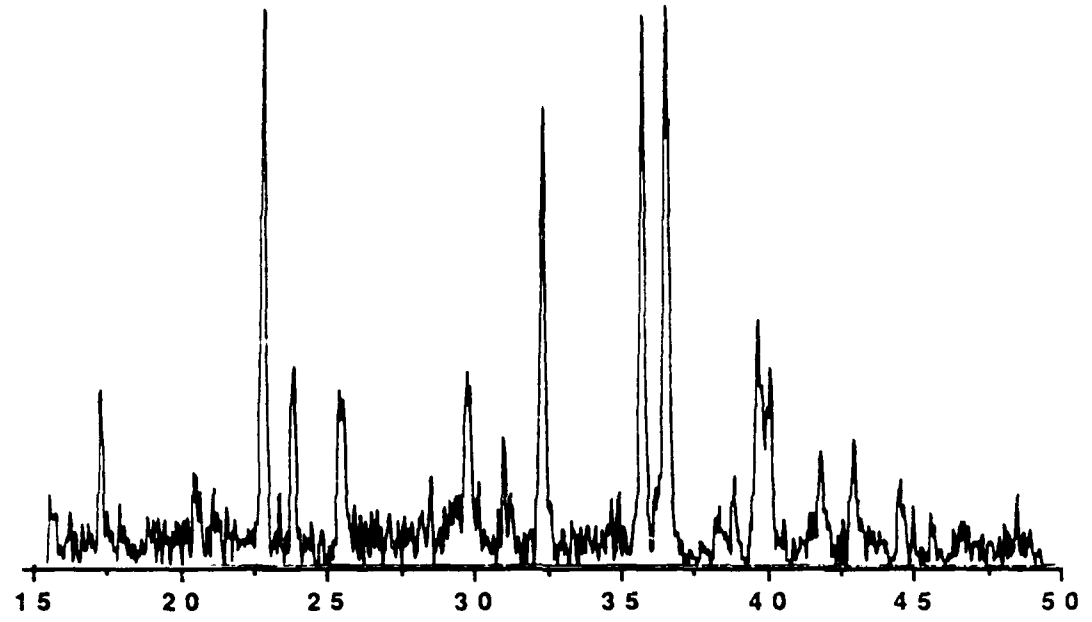
15 20 25 30 35 40 45 50
Degrees 2Ø

(b)

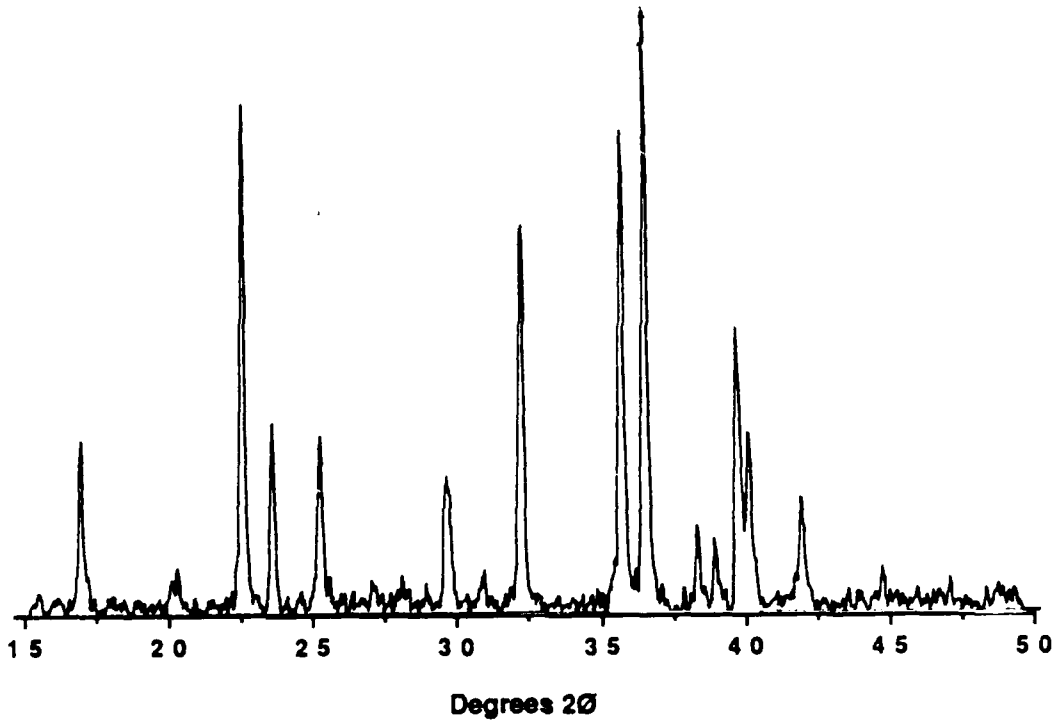
15 20 25 30 35 40 45 50
Degrees 2Ø

(a)

Figure 3.

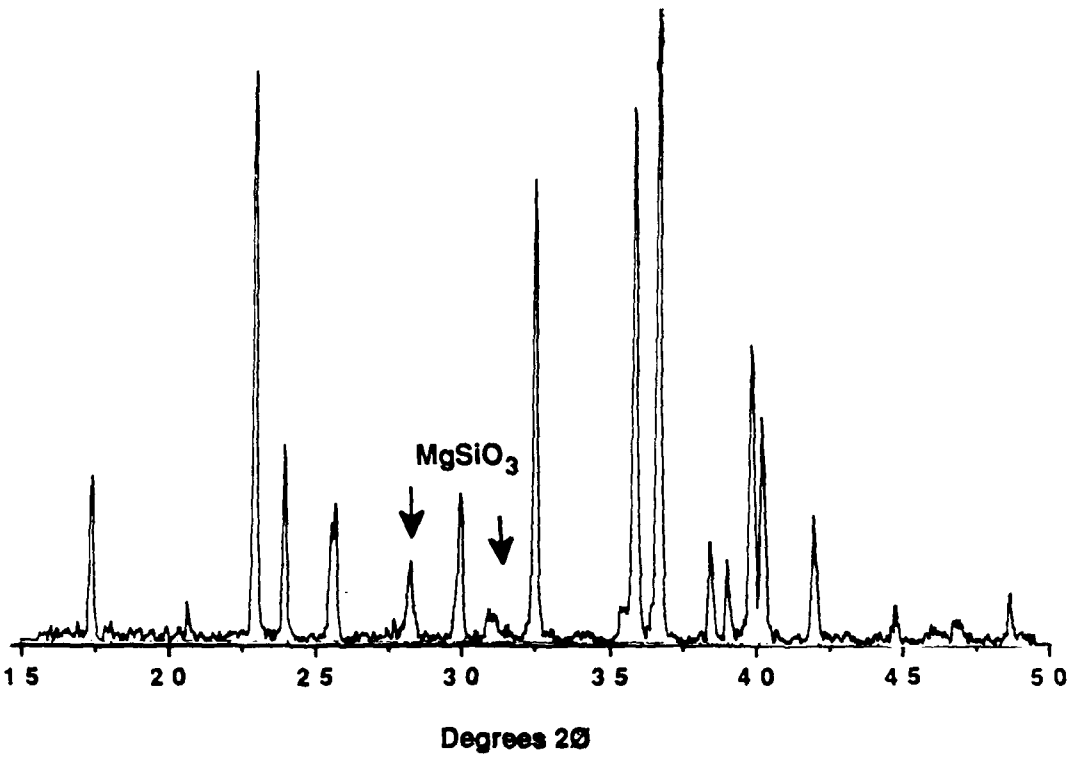

Figure 4.

MANUSCRIPT #4

Sol/Gel Processing of Si-O-C Glasses for Glass Matrix Composites

SOL/GEL PROCESSING OF Si-O-C GLASSES FOR GLASS MATRIX COMPOSITES

H. Zhang and C. G. Pantano
Department of Materials Science and Engineering
The Pennsylvania State University
University Park, PA 16802

INTRODUCTION

In earlier studies, the thermochemical interactions between carbon fibers and silicate glass matrices were evaluated.[1] It was found that at the processing temperatures where the molten glass matrix and the fiber surfaces are in contact, the predominant reactions produce CO, CO_2 and SiO gases. These reactions are greatly enhanced if the glass matrix composition contains variable valence and/or reducible oxides such as Nb_2O_5 or MoO_3. In these cases, it could be shown that significant degradation of the fiber surfaces occurs, and moreover, solid phase reaction products including Nb-carbide and Mo-carbide eventually form at the interface.[2] If excessive, these interphases lead to a measurable increase in the interfacial shear strength, and correspondingly, a decrease in the strength and fracture toughness of the composite.

On the basis of these observations, it was proposed that the reactions would be limited if *chemically-reduced* glass matrices were used in the composite fabrication; that is, glasses whose redox potential has been equilibrated with carbon. In this way, a great deal of latitude would exist in the time and temperature schedule for hot pressing. Further, it might be possible to improve the oxidation resistance of the composite because the matrix would oxidize in preference to the fibers. In general, though, the ability to control the interfaces through the redox potential of the glass matrix phase would represent a new approach to tailoring the interface properties in composites. One way to reduce the oxidation state of the glass is to substitute carbon for oxygen in the silicate network.

We have already developed a sol/gel method for the synthesis of glasses and glass matrix composites.[3] This approach has been extended to synthesize glass matrix materials which are chemically reduced and/or enriched in carbon. The sols are prepared using organometallic silanes

which contain one unhydrolyzable alkyl group. In this way, carbon can be retained in the gel, and most importantly, some of the carbon is covalently bonded to silicon. The gel can then be processed in an inert atmosphere to create a carbon-containing x-ray amorphous *black glass*. The gel can be processed to yield a glass frit for conventional composite processing, or it can be used directly to pre-preg fiber tape or paper.

The reduced state of this *black glass*, and its high temperature stability, are dependent upon the existence of Si-C bonds – that is, an oxycarbide network. The presence of a fine scale second phase of amorphous carbon would not be objectionable provided it was in equilibrium with the oxycarbide network. According to Pampuch, et al.,[4-6] a ternary Si-O-C phase can be observed during the oxidation of SiC, but due to its thermal instability, it is confined to the interface region of the oxide scale. The objective of this study is to create this metastable ternary Si-O-C phase through the heat-treatment of silicate gels which contain alkyl groups ($\equiv Si\text{-}C_xH_{2x+1}$).

The sols were prepared using four different organometallic precursors – methyl, ethyl, propyl and phenyl trimethoxysilanes. The hydrolysis of the silanes was studied using ^1H nuclear magnetic resonance (NMR). The gels were then characterized using carbon chemical analysis, and both ^{29}Si and ^{13}C magic-angle spinning NMR (MAS-NMR). The heat treatment of those gels to create a *black glass* was followed using thermal gravimetric analysis (TGA), and the final characteristics of the glass were determined using chemical analysis, x-ray photoelectron spectroscopy (XPS) and both ^{29}Si and ^{13}C MAS-NMR. Although the reduced black glasses to be used in composites will be borosilicate compositions, these basic studies of hydrolysis and structure were carried out using pure silicates.

EXPERIMENTAL PROCEDURE

The silanes listed in Table I were hydrolyzed using water and HCl catalyst. Each of the silanes was mixed with ethanol and then either 2, 4, 6, or 8 moles of H_2O (per mole of silane) was added. The solution was adjusted to pH 3 using the 1M HCl. The mixture was stirred on a hot plate at 60-80°C for four hours. In selected preparations, solution was extracted for ^1H NMR

analysis. Otherwise, 2M NH_4OH was added to initiate gelation. At pH 8, the gelation was complete in ~48 hours at room temperature. After drying at 85-90°C for seven days, a stiff, transparent gel was obtained. The gels were subsequently heat-treated in a tube furnace at 900°C under flowing argon. This yielded large fragments of silica *black glass*.

A borosilicate *black glass* was synthesized via a sol/gel synthesis with the composition: 78%SiO_2, 13%B_2O_3, 3%C, 2% Al_2O_3 and 4% Na_2O (by weight). The sol was prepared in a manner identical to that already reported[3] except that one-half of the tetraethoxysilane was replaced by methyltrimethoxysilane. This sol was used to prepare a carbon-fiber paper reinforced composite also according to the method already reported.[3] The dried gel composite was heat-treated at 600°C in Ar, and then hot-pressed at 1200°C in vacuum.

The carbon content of the gels and glasses was determined using a LECO Carbon Analyzer. The thermal stability of the gels and glasses was studied using a Dupont Instruments 2100 Thermal Analyzer.

The hydrolyzed solutions, gels and black glasses were characterized using nuclear magnetic resonance (NMR). In the case of the solutions, a Bruker 300 AM NMR spectrometer was used to obtain ^1H spectra; the sols were diluted with deuterated methanol. The ^{29}Si and ^{13}C spectra of the gels and glasses were obtained using MAS-NMR on an Oxford Instrument with a Probe Systems, Inc. magic-angle spinning probe.

The structure of the glasses was further characterized using x-ray photoelectron spectroscopy (XPS), but these data are not included in this report.

RESULTS AND DISCUSSION

Hydrolysis

The extent of hydrolysis in the various solutions was determined using proton (^1H) NMR. The ^1H NMR spectra can distinguish hydrogen in the alkyl and alkoxy ligands of the silane molecules. It can also fingerprint the hydrogen in hydroxyl groups, but the presence of alchohol and water in the solution prevents any definitive analysis of hydroxyls in the silane itself. Here, it

could be assumed that decreases in the intensity of the ^{1}H NMR line due to the alkoxy (or alkyl) groups would be indicative of hydrolysis.

These NMR experiments were carried out using the propyltrimethoxysilane solutions only. The solutions were prepared with 0, 2, 4, 6 or 8 moles of water (per mole of silane). In the unhydrolyzed solution, a line for the methoxy group (Si-O$\underline{CH_3}^{d}$) was clearly evident at 3.535 ppm, and a triplet of lines for the ethyl (Si-$\underline{CH_2}^{a}$-$\underline{CH_2}^{b}$-$\underline{CH_3}^{c}$) was found downfield at 1.424 (a), 0.615 (b), and 0.970 (c) ppm. This is shown in Figure 1a. In the hydrolyzed solutions, a significant decrease in the intensity of the methoxy line at 3.535 ppm occurred (see also Figure 1a). The ratio of intensities for the methoxy-d and propyl-c lines is plotted in Figure 1b against the moles of water used in the various solutions. The ratio is a quantitative measure of the various states of hydrogen in the silane molecule. It is 3.00 in the unhydrolyzed solution because the precursor molecule has three methoxy groups and one propyl group. The decrease in this ratio is due to hydrolysis of the methoxy groups. It can be seen that most of the hydrolysis occurs with only 2 moles of water per mole of silane, and that further increases in water concentration exhibit a negligible effect. In all cases, >95% of the methoxy groups have been hydrolyzed. But the most important implication of these data is the persistence of the alkyl group in the hydrolyzed silane (lower spectra in Figure 1a), or more specifically, the Si-C bond associated with the hydrolyzed silane $(OH)_3Si\text{-}CH_2CH_2CH_3$.

Carbon Analyses

The gels and black glasses (synthesized with 6 moles of water per mole of silane) were subjected to a chemical analysis to determine the total carbon content. The results are presented in Table I. In the gels, the carbon content increases with the chain length of the alkyl group. There is an obvious quantitative relation between the composition of the unhydrolyzed silane precursors and the carbon content of the various gels. This is consistent with complete hydrolysis of the methoxy groups (and some condensation) but retention of the alkyl group; i.e., $[CH_3O]_3SiR+H_2O\rightarrow OH(O_{2/2})SiR+3CH_3OH$. The condensation of two hydroxyl groups per silane molecule in the gel was established on the basis of ^{29}Si NMR (see below).

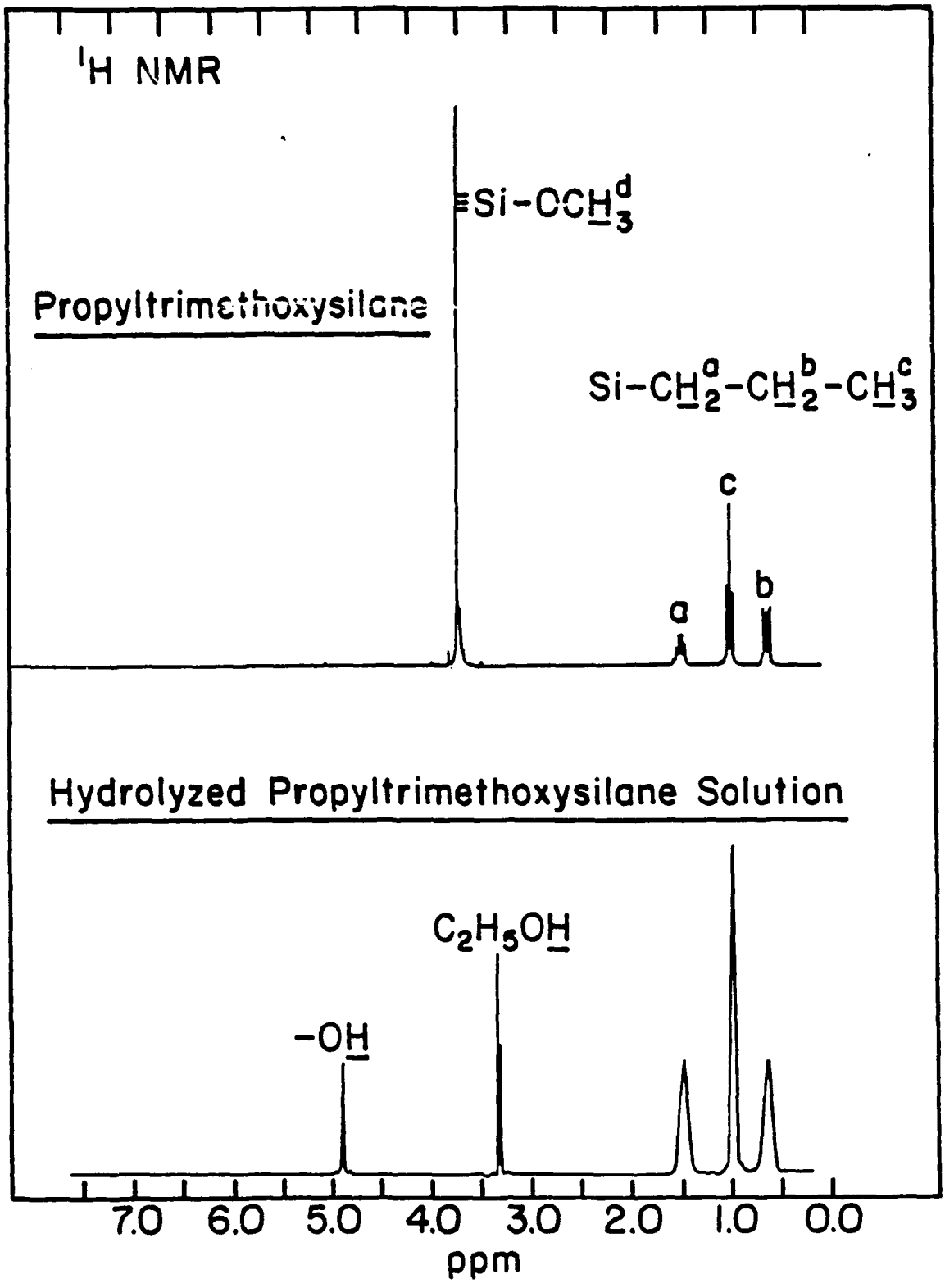

Figure 1a. ^{1}H NMR spectra of unhydrolyzed precursor (upper) and solution hydrolyzed with 8 moles of water (lower).

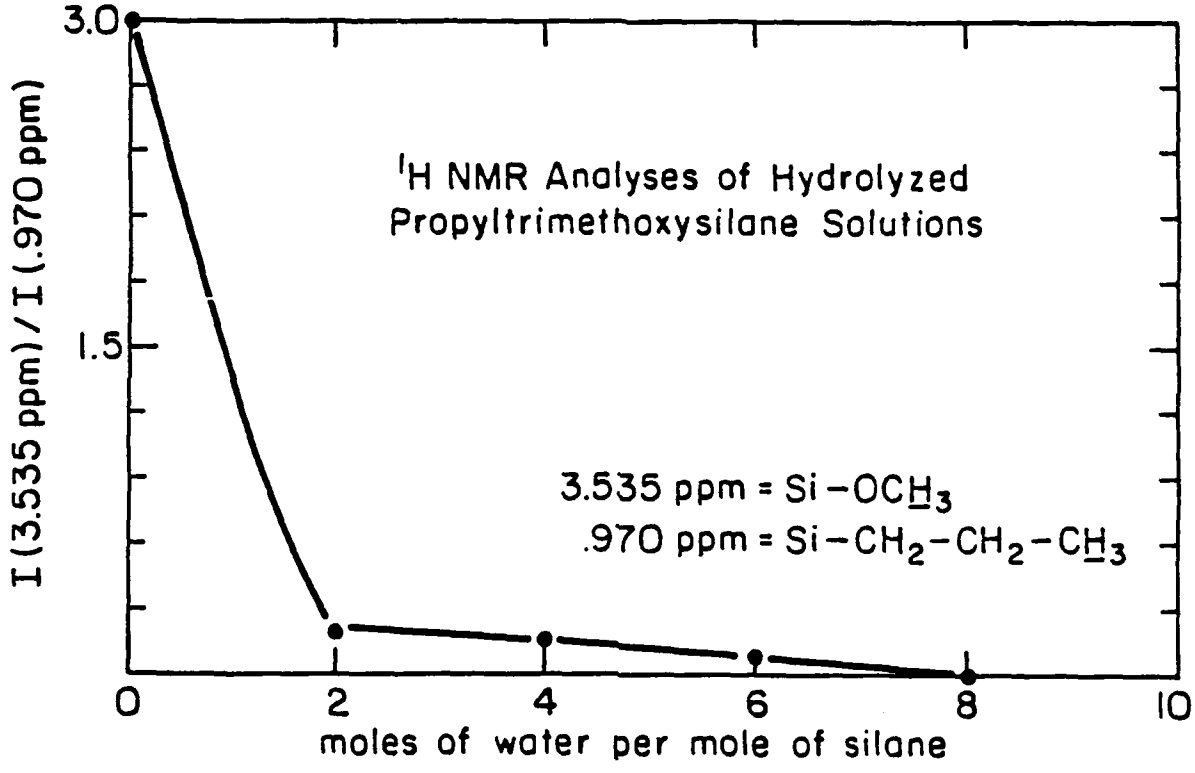

Figure 1b. The intensity ratio of the methoxy to propyl ^{1}H NMR lines.

Table 1

Precursor[1]	Composition	Total % Carbon (calculated)	% Carbon after hydrolysis[3] (calculated)[2]	% Carbon in gel (measured)[3]	%Carbon in glass (measured)[3]
methyltrimethoxysilane	$CH_3Si(OCH_3)_3$	35	16	14	12
ethyltrimethoxysilane	$C_2H_5Si(OCH_3)_3$	40	27	24	17
propyltrimethoxysilane	$C_3H_7Si(OCH_3)_3$	44	34	32	18
phenyltrimethoxysilane	$C_6H_5Si(OCH_3)_3$	54	52	57	41

1 Petrarch Systems, Inc., PA, USA
2 Calculated assuming hydrolysis and condensation to $OH(O_{2/2})SiR$ where R = alkyl
3 Leco Carbon Analysis

After the high temperature heat treatment, though, the carbon content is reduced to a level which appears insensitive to the carbon content of the precursor. This implies that increasing the chain length of the alkyl group does not introduce any more carbon into the glass. If it is assumed that only the carbon atom bonded to the silicon atom can be retained in the glass, the expected glass composition would be $SiO_{3/2}C$. This corresponds to a carbon content of ~19%. This is close to the observed range of 12-18% in the glasses. The glass prepared with the phenyl-silane is an exception to this hypothesis, probably because the bulky benzene ligand influences condensation of the gel. The phenyl-derived-gels and glasses behave and appear different than the simpler methyl, ethyl and propyl gels and glasses.

Thermal Stability

The gels and glasses were subjected to a variety of TGA analyses. In the case of the gels, the weight losses expected due to carbonization of the alkyl groups are 16, 27, 34 and 52 for methyl, ethyl, propyl and phenyl, respectively (again, assuming $OH(O_{2/2})SiR$ in the gel). Figure 2 shows that these calculated weight losses are in excellent agreement with the weight loss measured during thermal decomposition in air. This further verifies the nearly complete hydrolysis of the methoxy groups, and correspondingly, the persistence of the alkyl groups in the dry gels. Figure 3a shows that the amount of weight loss is relatively independent of the water content in the solution. This is consistent with the ^1H NMR data in Figure 1, and again, verifies nearly complete hydrolysis of the methoxy groups.

TGA of the dry gels was carried out in argon to evaluate the weight loss behavior during conversion of the gel to black glass. Figure 3b is the data for the propyl-silane gel. Here, the weight change is due to the loss of carbon and hydrogen (in the alkyl groups) as well as oxygen (in the silicate gel network). The evolution of CO, CO_2, CH_3 and H_2O during heat-treatment in argon was verified using a CO_2 coulometer cell. The weight loss due to carbon was about 18%. Clearly, this carbonization of the alkyl groups – in argon – occurs through a carbothermic reduction of the silicate network. This probably accounts for the difference in carbonization

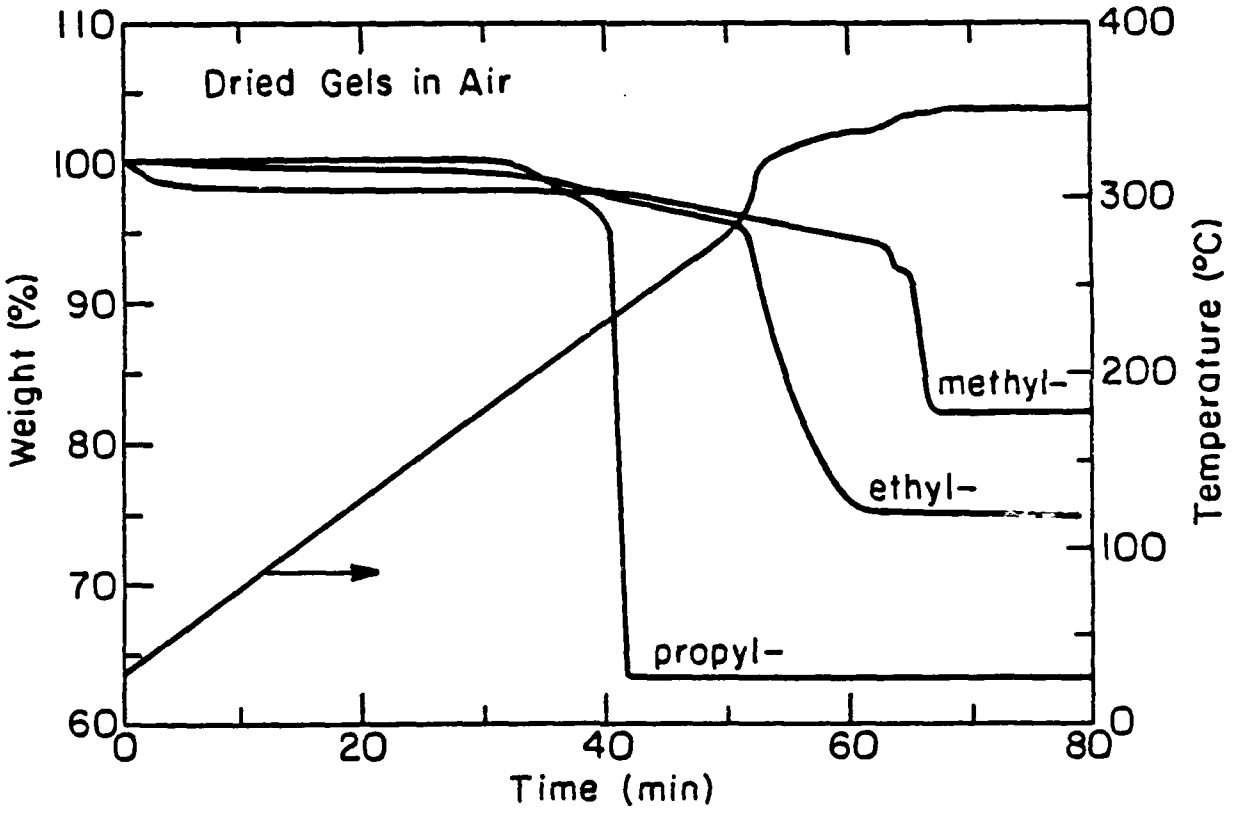

Figure 2. The weight loss (TGA) in air for methyl-, ethyl- and propyl-trimethoxysilane gels.

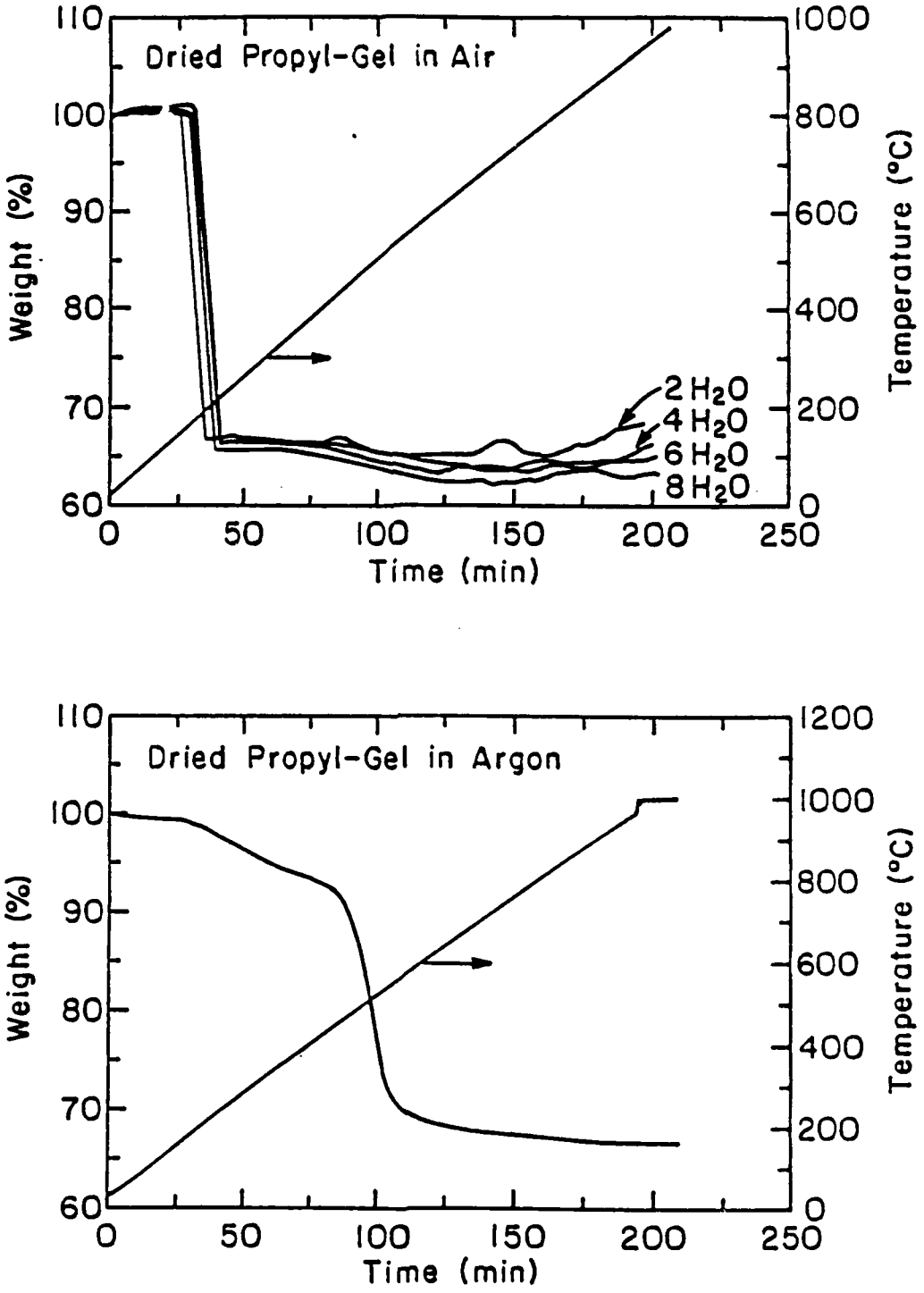

Figure 3. The weight loss (TGA) in air (upper) and in argon (lower) for propyl-trimethoxysilane gels; the analyses of gels prepared with different water concentrations is also shown (upper).

temperature in air versus argon (compare Figures 3a and 3b). Presumably, the activation energy for carbonization by O_2 is less than that for carbothermic reduction of SiO_2.

Finally, TGA of the *black glasses* was carried out in air and in argon to determine the stability of the carbon in the dense glass structure. These glasses were prepared by heat-treatment of the gels in argon at 900°C; the carbon contents of these black glasses is reported in Table I. The data in Figure 4 shows that no significant weight loss is observed at temperatures up to 1000°C over time periods up to two hours. This is due to the thermodynamic stability of the Si-C bonds present in the structure, and in the case of heat-treatment in air, to the kinetic limitations of oxygen diffusion. This stability was observed in the methyl, ethyl and propyl derived glasses.

Structure

The ^{13}C NMR and ^{20}Si NMR spectra provided the most definitive characterization of the gel and glass structures. Figure 5 shows the ^{13}C NMR spectra of the various dry gels. Each spectra shows a single line or group of lines which is due to the alkyl group. The important observation is the absence of a line due to the carbon in methoxy groups which is observed in the corresponding ^{13}C spectra of the various precursors at ~50 ppm. This conclusion is consistent with the ^{1}H NMR analyses of the solutions and the TGA analyses of the dry gels. And because ^{29}Si NMR cannot distinguish between Si-OH and Si-OCH_3, this data facilitates assignment of the ^{29}Si resonance (see below), i.e., it eliminates the possibility of Si-OCH_3.

Figure 6 compares the ^{29}Si NMR spectra for the gel and glass prepared using the methyl-trimethoxysilane. The spectra for the methyl-trimethoxysilane precursor is included for reference. In contrast to the sharp line characteristic of the monomeric precursor, the polymeric gel yields a broadened spectra with two distinct lines.

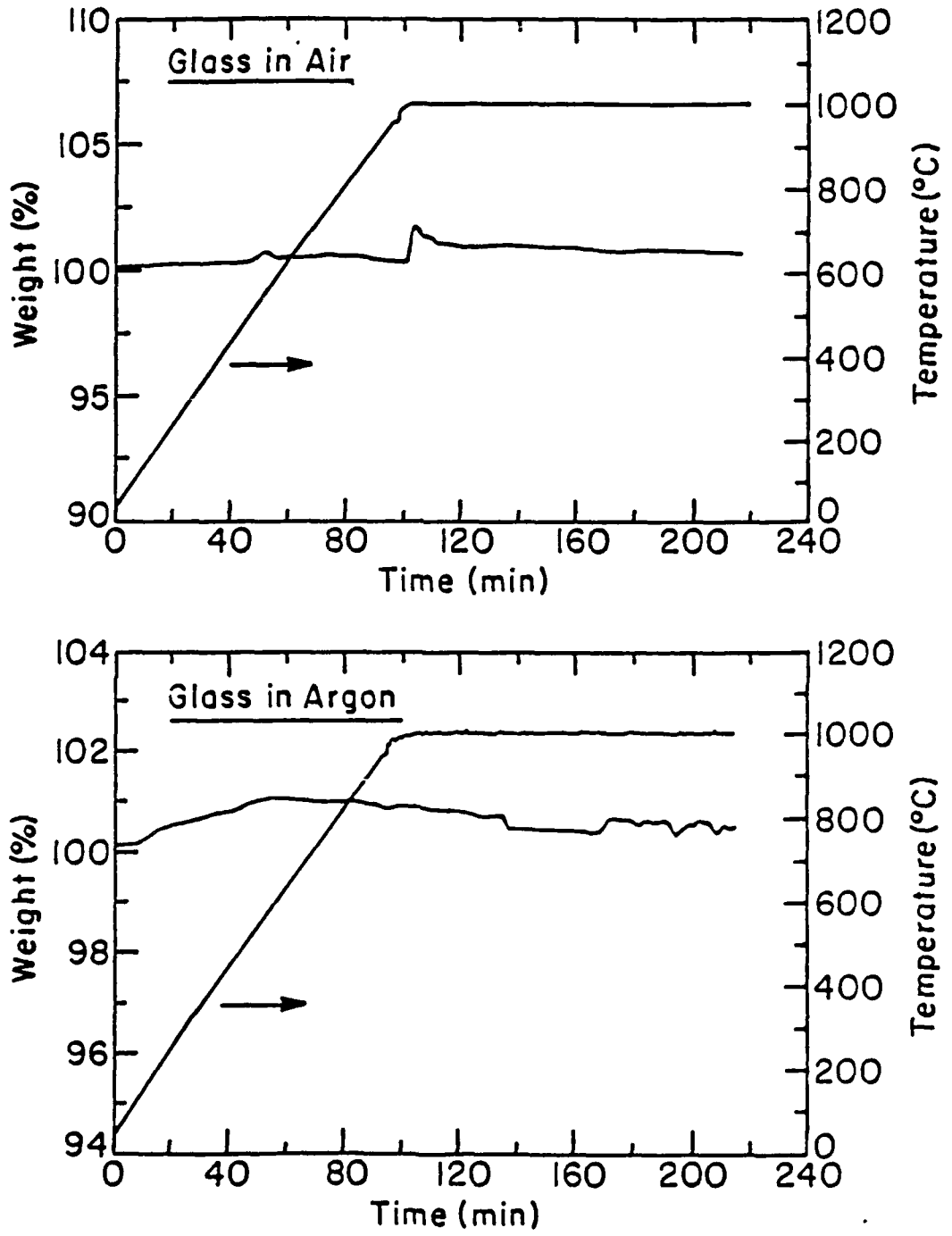

Figure 4. The weight loss (TGA) for *black glasses* in air (upper) and argon (lower); these glasses were obtained after heat-treatment of a methyl-gel in argon at 900°C.

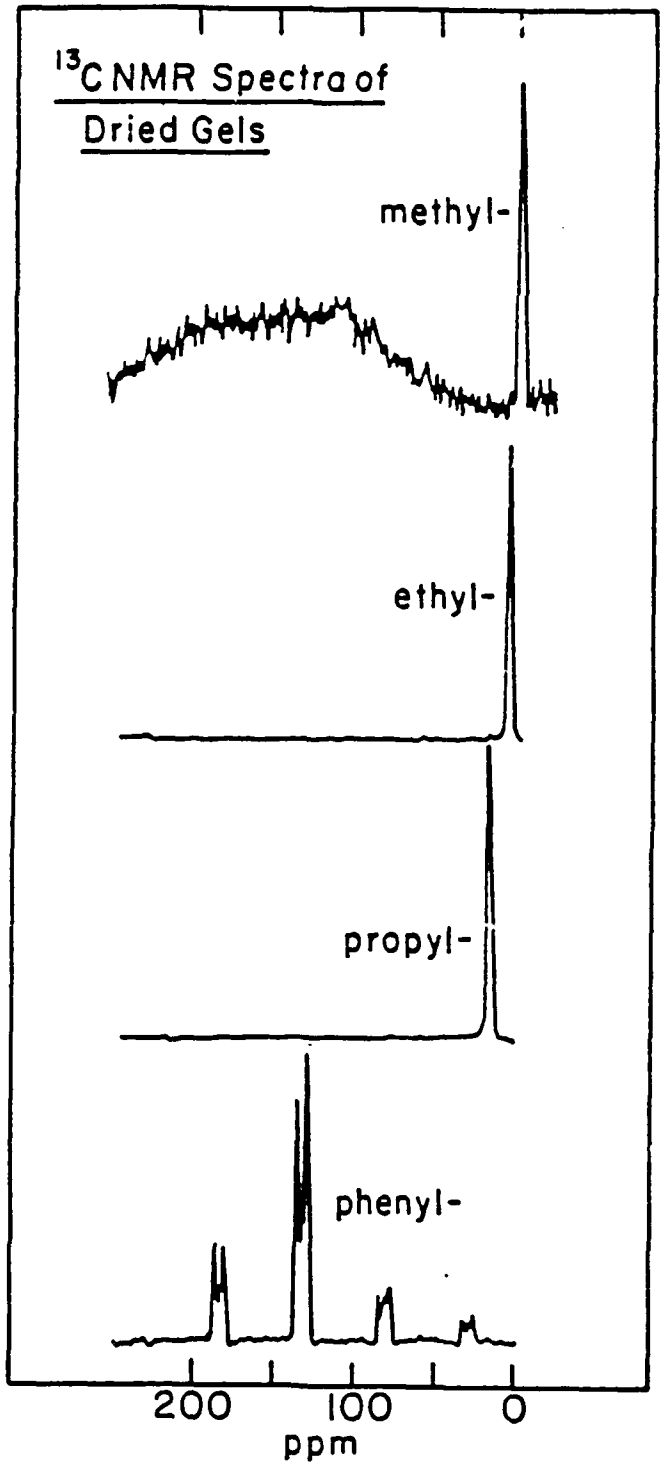

Figure 5. The ^{13}C NMR spectra of dry gels show lines for the carbon atoms in the alkyl-groups; the lines due to carbon in the methoxy groups (~50 ppm) are not observed in the gels.

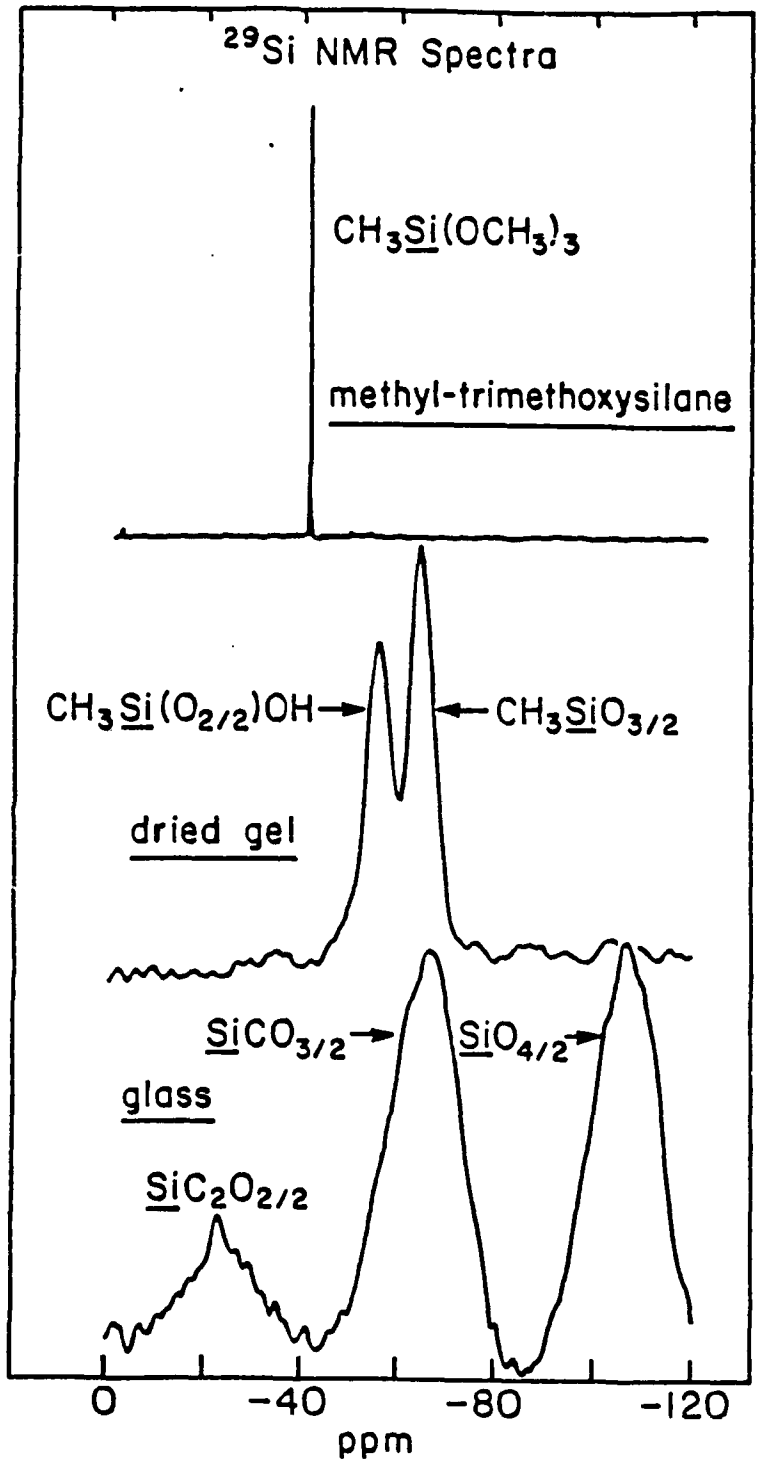

Figure 6. ^{29}Si NMR spectra of the methyl-trimethoxysilane precursor, dry gel, and *black glass*.

The line at ~-56 ppm is due to $RSi(O_{2/2})OH$:

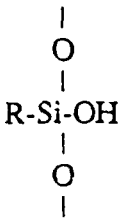

and the line at ~-66 ppm is due to $R\ SiO_{3/2}$:

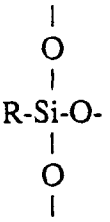

These assignments are based upon data in the literature[7-11] for model silane compounds, and the ^{13}C NMR data presented above. The spectra in Figure 7 show that these two configurations exist in all the dry gels. The minor differences in the peak positions are due to the shielding effects of the different alkyl groups.

The *black glasses* yield ^{29}Si NMR spectra which are broadened. The main peak occurs at the resonance position for $[SiO_{4/2}]$ (~110 ppm) but there are at least two other silicon configurations. One is due to $[SiCO_{3/2}]$ and the other $[SiC_2O_{2/2}]$. These assignments are also based upon data for model silane compounds,[7-11] as well as silica and silicon-carbide. It is clearly evident that Si-C bonds are present within the polymerized silicate glass network. Figure 8 shows that the distribution and relative concentration of the various Si-configurations are nearly equivalent for the methyl-, ethyl- and propyl-precursors. There is approximately 40-45%$[SiO_4]$, 40-45%$[SiCO_{3/2}]$ and ~15%$[SiC_2O_{2/2}]$. What is not clear is the configuration of carbon within the silicon oxycarbide network. Although the ^{29}Si spectra verify the presence of Si-C bonds, it does not indicate whether this carbon is terminal or cross-linked. In principle, ^{13}C NMR could provide this information, but the spectra obtained for the glasses were broad and complex. The ^{13}C NMR spectra of the glasses do suggest the presence of amorphous carbon.

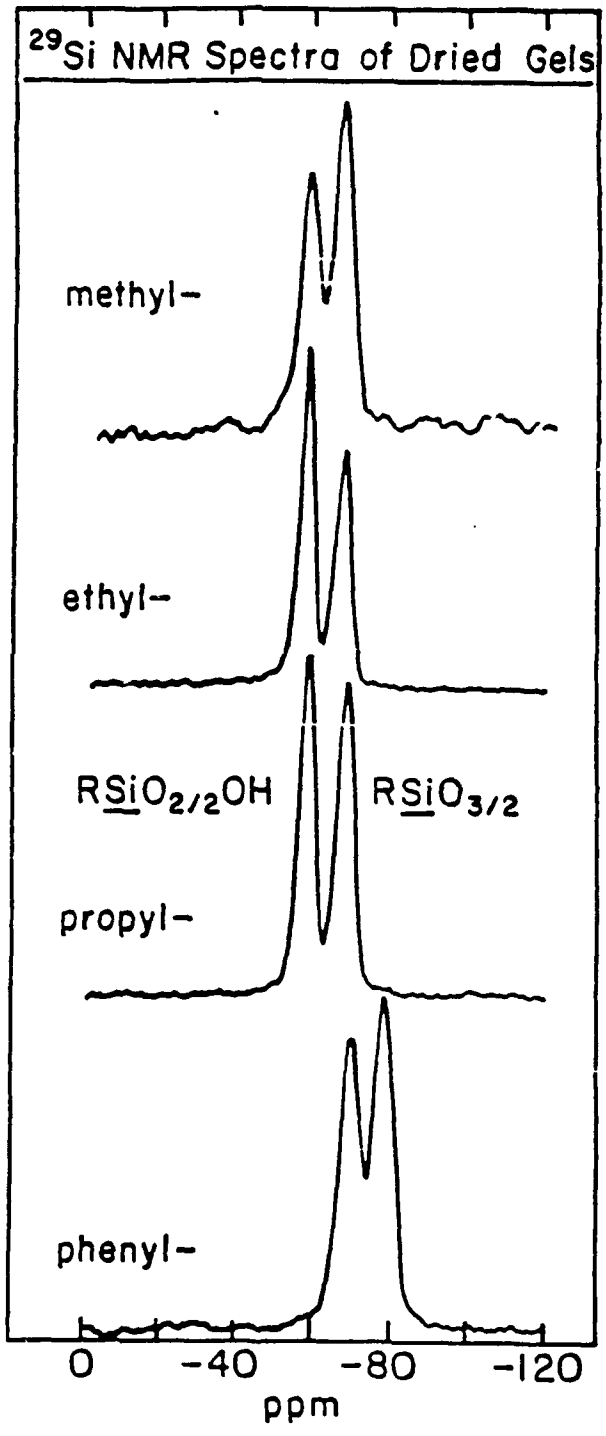

Figure 7. ^{29}Si NMR spectra of the dry gels prepared with methyl-, ethyl-, propyl- and phenyl-trimethoxysilane; in all cases, one line is due to R $SiO_{3/2}$ and the other R $Si(O_{2/2})OH$ (where R = methyl, ethyl, propyl or phenyl).

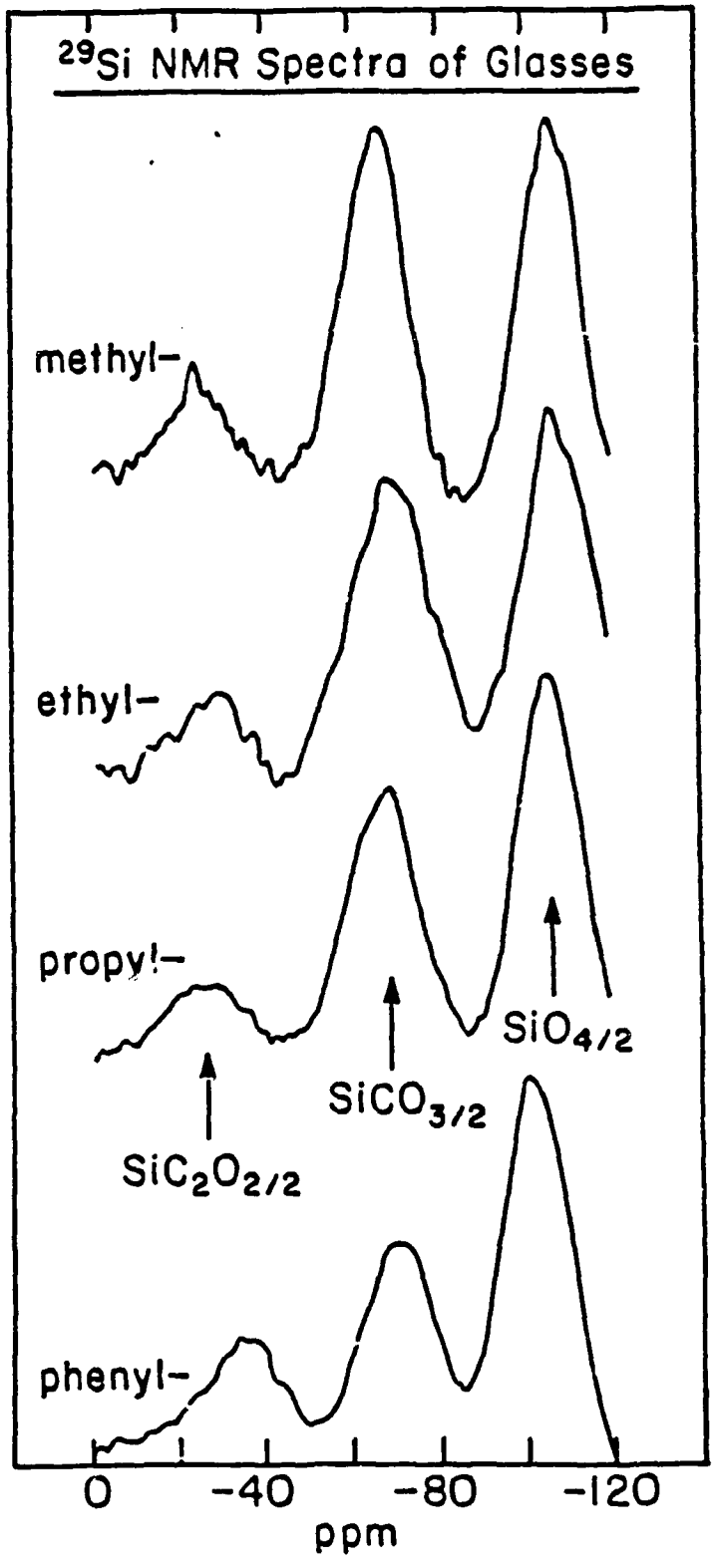

Figure 8. ^{29}Si NMR spectra of the *black glasses* prepared using methyl-, ethyl-, propyl- and phenyl-trimethoxysilanes.

SUMMARY

It has been shown that x-ray amorphous glasses – containing up to 18% carbon – can be synthesized using a sol/gel process. Most importantly, though, Si-C bonds are found in the glasses prepared by heat-treating the gels at high temperature in an inert atmosphere; i.e., the synthesis does, in fact, create an *oxycarbide* structure.

^{1}H NMR, ^{13}C NMR and TGA revealed that the methoxy groups in methy, ethyl, propyl and phenyl trimethoxysilanes are hydrolyzed in the solutions, and therefore, absent in the gels. But the alkyl groups are retained in the dry gels. The ^{29}Si NMR data verified that the Si-C bonds associated with these alkyl groups are intact in the dry gels.

The amount of carbon in the gel is dependent upon the carbon content of the alkyl group in the precursor, but the carbon content in the glass is limited to 12-18%. Thus, it is proposed that only the carbon atom bonded directly to the silicon can be retained in the glass structure. The other carbon atoms in the alkyl chain of the gel probably react with hydroxyl and silicate species to evolve CO and CO_2 and/or to precipitate amorphous carbon second phase particles. Of course, the reactions must be more complex than this because some fraction of the Si species in the glass were found to have two carbon ligands. Until the bonding and cross-linking of these carbon ligands in the glass are fully characterized, this issue will be uncertain. Nevertheless, these data suggest that the methyl-trimethoxysilane is the most appropriate oxy-carbide glass precursor unless excess amorphous carbon (second-phase) is desired in the microstructure. The ^{13}C NMR did suggest the presence of amorphous carbon in the glasses, but its concentration, distribution and effect upon the glass properties has not yet been determined.

The TGA analyses of glasses – in air – revealed that these materials are oxidation resistant to 1000°C. The oxidation of SiC occurs in the range 500-1000°C, and this provides a sense of thermodynamic stability to the glass. And since oxygen must diffuse through the glass to oxidize the Si-C bonds, a measure of kinetic stability is also provided.

The synthesis has been successfully applied to the fabrication of carbon fiber reinforced composites. In this case, borosilicate glass (Pyrex composition) matrices were synthesized using

methyltrimethoxysilane rather than tetraethoxysilane. It remains to be determined whether the properties and interface chemistry in these new oxycarbide glass matrix composites offer advantages over their pure oxide counterparts. Similarly, the physical properties of the oxycarbide glasses, themselves, have not yet been measured. Certainly, the hardness, thermal expansion, elastic modulus and glass transition temperatures should be influenced by the substitution of C for O.

REFERENCES

1. P. Benson, K. E. Spear and C. G. Pantano, in Ceramic Microstructure '86, J. A. Pask and A. G. Evans, Eds. (Plenum, New York, 1987), pp. 415-426.
2. W. K. Tredway, K. M. Prewo and C. G. Pantano, to appear in Carbon, 1989.
3. D. Qi and C. G. Pantano, Ultrastructure Processing of Advanced Ceramics, J. D. MacKenzie and D. R. Ulrich, Eds. (Wiley, New York, 1988), pp. 635-649.
4. R. Pampuch, S. Jonas and J. Stoch, Science of Ceramics, 9, 300-307 (1977).
5. V. A. Lavrenko, S. Jonas and R. Pampuch, Ceramics International, 2, 75-76 (1981).
6. R. Pampuch, W. S. Ptak, S. Jonas and J. Stoch, Proceed. 9th Inter. Symp. Reactivity of Solids, 674-677 (1980).
7. D. A. White, S. M. Oleff and J. R. Fox, Advanced Ceramic Materials, 2(1), 45-53 (1987).
8. D. A. White, S. M. Oleff and J. R. Fox, Advanced Ceramic Materials, 2(1), 53-59 (1987).
9. G. E. Maciel, M. J. Sullivan and D. W. Sindorf, Macromolecules, 14, 1607-1608 (1981).
10. D. W. Sinderf and G. E. Maciel, J. Am. Chem. Soc., 105, 3767-3776 (1983).
11. J. Lipowitz, H. A. Freeman, R. T. Chen and E. R. Prack, Advanced Ceramic Materials, 2(2), 121-128 (1987).
12. R. Pampuch, W. Patal:, S. Jonas and J. Stoch, Proceed. 4th CIMTEC St. Vincent, P. Vincenzini Ed. (Elsevier Publ., Amsterdam, 1980) pp. 435-448.